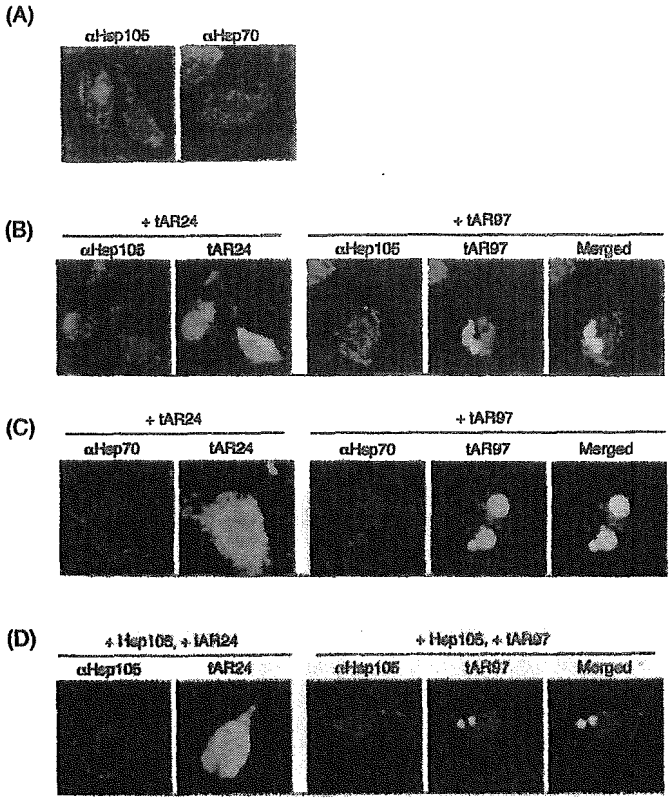

FIG. 3. **Localization of Hsp105α and Hsc70/Hsp70 in COS-7 cells with tAR97 aggregates.** *A*, control COS-7 cells were fixed, and endogenous Hsp105α (*red*) or Hsp70 (*red*) was detected by indirect immunofluorescence using anti-Hsp105 or anti-Hsp70 antibody, respectively. Nuclear morphology (*blue*) was detected by staining with Hoechst 33342. *B* and *C*, COS-7 cells were transfected with the expression plasmid for tAR24 (+ *tAR24*) or tAR97 (+ *tAR97*) and incubated further for 72 h. tAR24 or tAR97 (*green*) was detected by the green fluorescence of GFP, and endogenous Hsp105α (*red*) (*B*) and Hsp70 (*red*) (*C*) were detected by indirect immunofluorescence. Nuclear morphology (*blue*) was observed by staining with Hoechst 33342. *D*, COS-7 cells were cotransfected with expression plasmids for Hsp105α and tAR24 (+ *Hsp105*, + *tAR24*) or Hsp105α and tAR97 (+ *Hsp105*, + *tAR97*) and incubated further for 72 h. Nuclear morphology (*blue*) stained with Hoechst 33342 and tAR97 (*green*) and Hsp105α (*red*) by indirect immunofluorescence was observed.

treated in formic acid for 5 min at room temperature and with trypsin (Dako) for 20 min at 37 °C. The tissue sections were blocked with normal goat serum (1:20) and incubated with rabbit anti-mouse Hsp105 antibody (1:100). The sections were incubated with biotinylated goat anti-rabbit IgG (Vector Laboratories), and immune complexes were visualized using streptavidin-horseradish peroxidase (Dako) and 3,3′-diaminobenzidine (Dojindo) substrate and counterstained with methyl green. For the immunohistochemistry of tissues of SBMA patients, paraffin-embedded sections of the spinal cord and scrotal skin from nine patients with clinicopathologically and genetically confirmed SBMA (age 51–84 years, mean 64.3 years) were examined using rabbit anti-human Hsp105 antibody (1:100).

RESULTS

Aggregation of Truncated AR with an Expanded Polyglutamine Tract and Induction Apoptosis in COS-7 and SK-N-SH Cells—Truncated ARs containing 24, 65, or 97 polyglutamine repeats (tAR24, tAR65, or tAR97, respectively) were transiently expressed in non-neuronal (COS-7) and neuronal cells (SK-N-SH) (Fig. 1). Because these tAR constructs were connected with GFP at the C terminus, the cellular localization of these chimerical peptides was detected by fluorescence microscopy. tAR65 or tAR97, but not tAR24, aggregated in cytoplasm and/or nucleus in non-neuronal COS-7 cells as well as neuronal SK-N-SH cells, as shown previously in the neuronal Neuro2a cell line (29). Proportions of cells with aggregates increased depending on the incubation time after transfection and polyglutamine repeat length. Approximately 45 and 60% of GFP-positive cells had aggregates in the COS-7 and SK-N-SH cell lines, respectively, at 72 h after transfection of the expression plasmid for tAR97. Among the cells with aggregates of tAR97, intranuclear aggregates were detected in 40 and 8% of transfected COS-7 and SK-N-SH cells, respectively (data not shown).

Under these conditions, apoptotic cells with condensed chromatin were observed in 12 and 18% of all COS-7 cells expressing GFP at 48 and 72 h after transfection of the expression plasmid for tAR97, respectively (Fig. 2*A*). In contrast, cells expressing tAR24 showed little apoptotic morphology after the transfection (Fig. 2*A*). Most apoptotic cells had aggregates of tAR97 in the nucleus, whereas cells containing cytoplasmic aggregates exhibited few apoptotic features (Fig. 2*B*). Furthermore, when the presence of fragmented DNA was assessed by the TUNEL method, the cells with intranuclear aggregates, but not cells with cytoplasmic aggregates, were found to be positive (Fig. 2*C*). These findings suggested that the intranuclear aggregates induced apoptosis in COS-7 cells. Similar results were obtained with SK-N-SH cells (data not shown). Thus, although both non-neuronal and neuronal cells could be utilized as a cell model of SBMA, we used the COS-7 model for further study because the cells expressed the transfected plasmids markedly well.

Colocalization of Hsp105α and Hsp70 with Aggregates of Truncated AR—We next examined the cellular distribution of Hsp105α and Hsp70 in COS-7 cells by indirect immunofluorescence using anti-human Hsp105 and anti-Hsp70 antibodies. Under nonstressed conditions, endogenous Hsp105α and Hsc70/Hsp70 were localized mainly in the cytoplasm of cells (Fig. 3*A*). When tAR24 was transiently expressed in COS-7 cells, both endogenous Hsp105α and Hsp70 were also detected in the cytoplasm of the cells (Fig. 3, *B* and *C*). In contrast, when tAR97 was transiently expressed in COS-7 cells, endogenous Hsp70 was colocalized to the aggregates of tAR97, whereas endogenous Hsp105α was not. However, when overexpressed with tAR97 in cells, Hsp105α was colocalized to the aggregates of tAR97 (Fig. 3*D*), whereas Hsp105α was localized to the cytoplasm of cells in which tAR97 was not expressed. Thus, the increased amounts of Hsp105α in cells seemed necessary for the interaction with and binding to the tAR containing an expanded polyglutamine tract.

Overexpression of Hsp105α Reduced Aggregation of tAR97—Hsp105α prevents the aggregation of denatured protein *in vitro* (45) and suppresses apoptotic cell death induced by various forms of stress in neuronal PC12 cells (44). Because the overexpressed Hsp105α colocalized to intracellular aggregates of tAR97 (Fig. 3), we next examined the effects of Hsp105α on the aggregation of tAR containing an expanded polyglutamine tract. When expression plasmids for Hsp105α and tAR97 were cotransfected into COS-7 cells, the proportion of cells with tAR97 aggregates was reduced to ~50% of that transfected without Hsp105α (Fig. 4, *A* and *B*). Overexpression of Hsp70 or Hsp40 also suppressed the formation of aggregates similarly to Hsp105α, and Hsp70 and Hsp40 in combination suppressed the formation strongly. However, the suppression of aggregation by Hsp70 and Hsp40 was not enhanced by the coexpression of Hsp105α.

When cellular toxicity was analyzed by examining the nuclear morphology of cells stained with Hoechst 33342, numbers of apoptotic cells with condensed chromatin were found to be markedly reduced by coexpression of Hsp105α with tAR97 (Fig. 4*C*). Overexpression of Hsp70 and/or Hsp40 also suppressed apoptotic cell death caused by expression of tAR97. Furthermore, when various amounts of Hsp105α were coexpressed

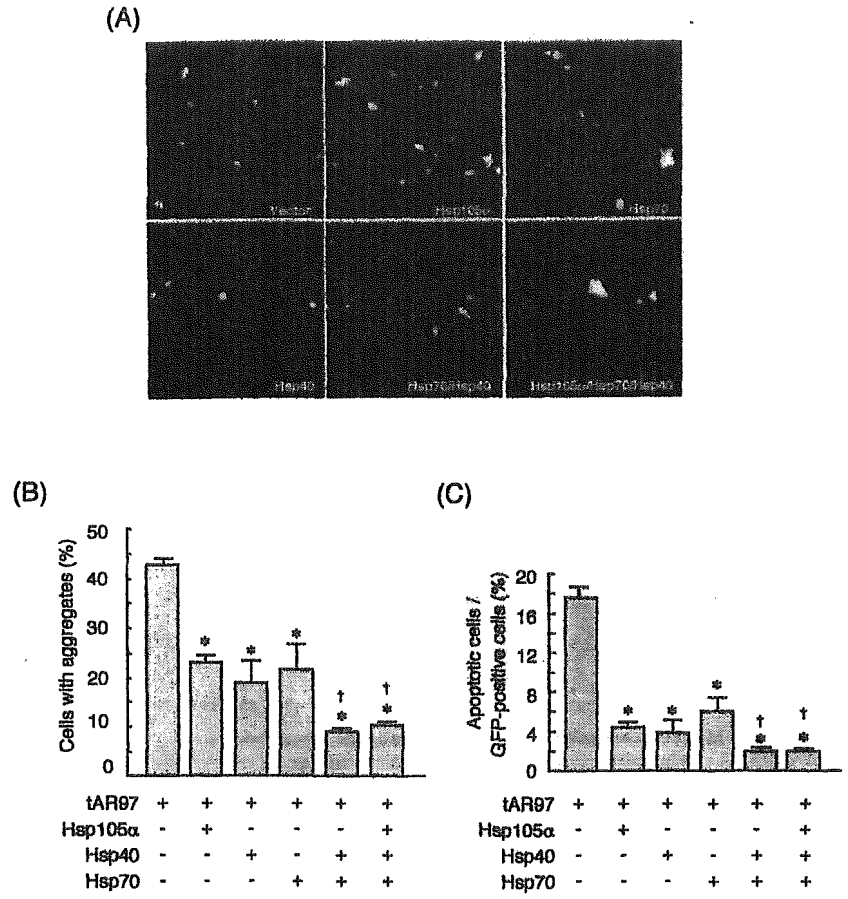

FIG. 4. **Effects of Hsp105α on aggregation of tAR97.** *A*, COS-7 cells were cotransfected with expression plasmids for tAR97 (0.5 μg) and pcDNA3.1 vector, Hsp105, Hsp70, and/or Hsp40 (1 μg each) and incubated further for 72 h. Typical images of fluorescence of GFP are shown. *B*, rates of cells with aggregates *versus* GFP-positive cells are shown. *C*, rates of apoptotic cells with condensed chromatin *versus* GFP-positive cells are shown. Values in *B* and *C* represent the mean ± S.D. of three independent experiments. Statistical significance was determined using Student's *t* test; *, $p < 0.01$ *versus* control with vector. †, $p < 0.01$ *versus* cells overexpressing Hsp70 or Hsp40 alone.

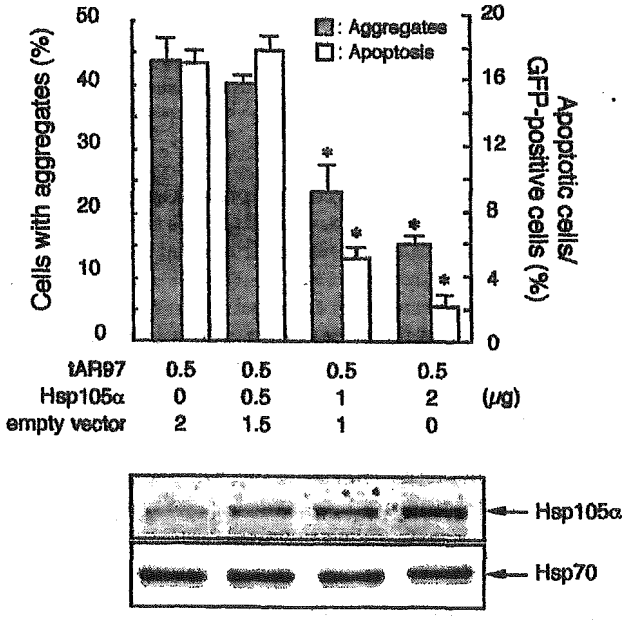

FIG. 5. **Hsp105α suppresses aggregation of tAR97 and cellular toxicity in a dose-dependent manner.** The expression plasmids for empty vector, Hsp105α, and/or tAR97 were introduced into COS-7 cells, and the cells were incubated further for 72 h. GFP fluorescence was observed using a confocal laser scan microscope. Rates of cells with aggregates or apoptotic cells/GFP-positive cells are shown as *closed* or *opened bars*, respectively. Values represent the mean ± S.D. of three independent experiments. Statistical significance was determined using Student's *t* test; *, $p < 0.01$ *versus* control with vector. *Lower panels* show Western blots of Hsp105α and Hsp70 in the cells.

with tAR97, the aggregation of tAR97 and apoptosis were both suppressed depending on cellular levels of Hsp105α (Fig. 5). Under these conditions, cellular levels of endogenous Hsp70 were not changed by overexpression of Hsp105α (Fig. 5, *lower panel*). These findings strongly suggested that when overexpressed, Hsp105α suppressed effectively not only the formation of aggregates but also the expanded polyglutamine-mediated cellular toxicity.

Identification the Domain of Hsp105α Required for Suppression of tAR97 Aggregation—Hsp105α is composed of N-terminal ATP binding, central β-sheet, loop and C-terminal α-helix domains, similar to the Hsp70 family proteins. To determine the domain of Hsp105α essential to suppress the aggregation caused by expansion of the polyglutamine tract, we constructed expression plasmids for various deletion mutants of Hsp105α, as shown in Fig. 6*A*. When coexpressed with tAR97 in COS-7 cells, the Hsp105α mutant C3 or ΔL significantly suppressed the aggregation of tAR97 as did wild-type Hsp105α (Fig. 6*B*). However, other deletion mutants failed to suppress the aggregation of tAR97. Because the C3 and ΔL mutants contain both β-sheet and α-helix domains, these domains seemed to be essential to suppress the aggregation caused by expansion of the polyglutamine tract.

Hsp105α Inhibits Aggregation of GST-tAR65 in Vitro—To examine further whether Hsp105α can directly suppress aggregation of the expanded polyglutamine tract, we analyzed the effects of Hsp105α on the aggregation of tAR65 *in vitro* (Fig. 7). GST-tAR65-HA was incubated with or without Hsp105α or its mutant, and insoluble aggregates that formed during the incubation were collected on cellulose acetate membranes. Hsp105α suppressed the aggregation of tAR65 in a dose-dependent manner (Fig. 7*A*). Furthermore, the aggregation was suppressed by wild-type Hsp105α and the mutants C3 and ΔL but not by other deletion mutants (Fig. 7*B*). Thus, it was suggested that Hsp105α itself suppressed the aggregation of truncated AR containing an expanded polyglutamine without other cellular components and that both the β-sheet and

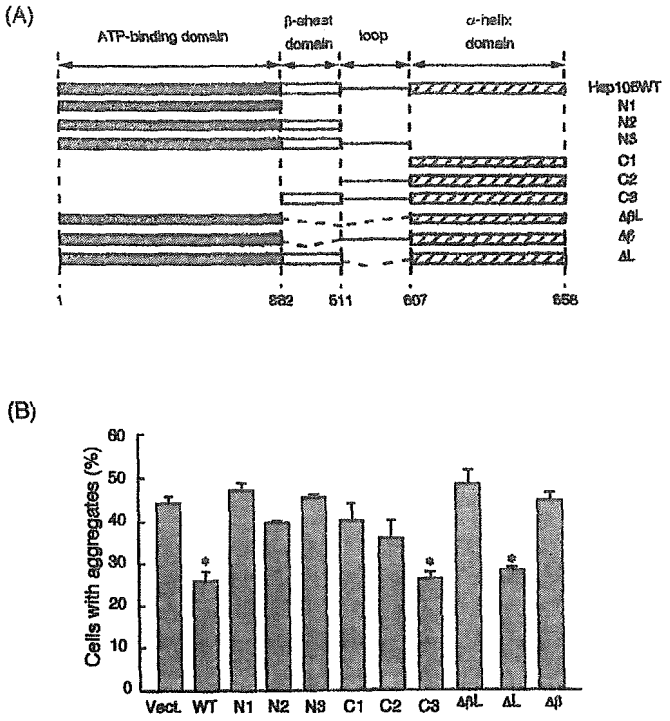

FIG. 6. **Domain of Hsp105α required for suppression of aggregation of tAR97.** *A*, schematic diagram of deletion mutants of Hsp105α. *B*, COS-7 cells were cotransfected with expression plasmid for tAR97 and deletion mutant of Hsp105α and incubated further for 72 h. GFP fluorescence was observed using a confocal laser scan microscope. Rates of cells with aggregates *versus* GFP-positive cells are shown. Values represent the mean ± S.D. of three independent experiments. Statistical significance was determined using Student's *t* test; *, $p < 0.01$ *versus* control with vector.

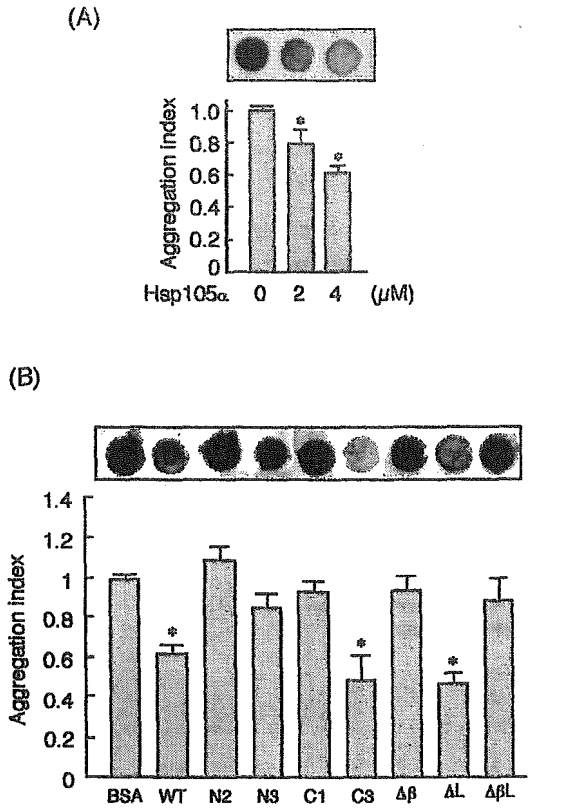

FIG. 7. **Hsp105α inhibits the aggregation of tAR65 *in vitro*.** *A*, 1 μM GST-tAR65-HA was incubated with 2 or 4 μM Hsp105α or 4 μM BSA at 25 °C for 16 h. *B*, 1 μM GST-tAR65-HA was incubated with Hsp105α, various deletion mutants of Hsp105α, or BSA (4 μM each) at 25 °C for 16 h. Then, aggregates were trapped on cellulose acetate membranes and detected by immunoblotting using anti-HA antibody. Densities of spots were quantified, and relative rates of tAR65 retained on membranes are shown as an aggregation index. Values represent the mean ± S.D. of three independent experiments. Statistical significance was determined using Student's *t* test; *, $p < 0.01$ *versus* control with BSA.

α-helix domains of Hsp105α seemed necessary for the suppression *in vitro* as well as *in vivo*.

Immunohistochemistry of Hsp105α in Nuclear Inclusions in the Tissues of SBMA Patients and Transgenic Mice—Nuclear inclusions containing mutant and truncated AR with an expanded polyglutamine have been shown to occur in residual motor neurons in the brain stem and spinal cord (4) and also in the skin, testis, and some other visceral organs of SBMA patients (5). We next examined whether Hsp105α localizes in the nuclear inclusions in these tissues of SBMA patients. As shown in Fig. 8, *A* and *B*, Hsp105α staining was observed in nuclear inclusions in neurons of the spinal anterior horn and scrotal skin epidermal cells. Furthermore, when male transgenic mice carrying a full-length AR with an expanded polyglutamine (97 repeats) tract and showing neuropathologic changes equivalent to human SBMA (49) were examined immunohistochemically, Hsp105α was also detected in nuclear inclusions in neurons of the spinal anterior horn and muscle cells (Fig. 8, *C* and *D*). However, although Hsp105α was commonly observed in nuclear inclusions in scrotal skin epidermal cells of SBMA patients and in muscle cells of the transgenic mice, only a few Hsp105-immunoreactive nuclear inclusions were observed in neurons of the spinal anterior horn of either patients or mice.

DISCUSSION

Hsp105α is a stress protein expressed at an especially high level in mammalian brain (43) and has an antiapoptotic effect in neuronal cells (44). Hsp105α prevents the aggregation of denatured proteins caused by heat shock *in vitro* but has not been shown to have chaperone activity (45). Here, we showed that Hsp105α suppressed not only the formation of intracellular aggregates but also apoptosis caused by an expansion of the polyglutamine tract in a cellular model of SBMA. Hsp105α is composed of N-terminal ATP binding, central β-sheet, loop, and C-terminal α-helix domains, similar to the Hsp70 family proteins. For the suppression of aggregation of truncated AR containing an expanded polyglutamine tract, β-sheet and α-helix domains of Hsp105α were essential *in vivo* and *in vitro*. Hsp70 binds unfolded proteins at the β-sheet domain and prevents aggregation of denatured proteins (50), and the α-helix domain is essential for stable binding to the substrate protein (50). Recently, we found that the β-sheet domain of Hsp105α could bind to denatured proteins.[2] Because Hsp105α mutants with β-sheet but not α-helix domains did not prevent the aggregation of truncated AR containing an expanded polyglutamine tract *in vivo* and *in vitro*, the α-helix domain may be necessary for stabilization of the Hsp105α-substrate complexes as is Hsp70.

Hsp70 and Hsp40 have recently been identified as important regulators of polyglutamine aggregation and/or cell death in cellular models of polyglutamine disease (29). Hsp70 promotes protein folding by an ATP-dependent process involving polypeptide segments enriched in hydrophobic residues (50, 51) and cooperates in this function with members of the Hsp40 family (52). The binding of Hsp70 to substrate proteins may prevent protein aggregation directly by shielding the interactive surfaces of nonnative polypeptides. Suppression of polyglutamine-induced neurotoxicity by expression of Hsp40 alone

[2] N. Yamagishi, K. Ishihara, and T. Hatayama, unpublished data.

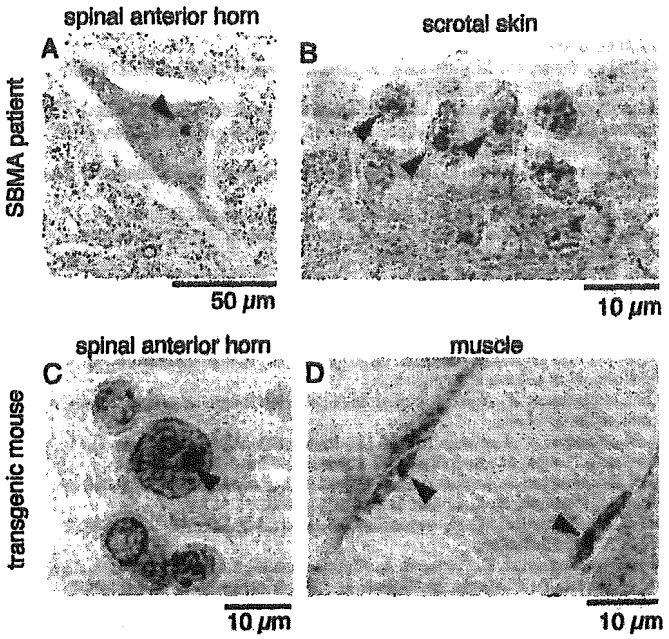

FIG. 8. **Immunohistochemistry of Hsp105α in nuclear inclusions in the tissues of patients and transgenic mice with SBMA.** Tissue sections of spinal anterior horn (*A*) and scrotal skin (*B*) from SBMA patients or spinal anterior horn (*C*) and muscle (*D*) from male AR-Q97 transgenic mice were examined using anti-human Hsp105 or rabbit anti-mouse Hsp105 antibody, respectively, and counterstained with methyl green. *Arrowheads* indicate nuclear inclusions.

is most likely caused by the ability to activate the endogenous Hsp70 for suppression of the neurotoxicity. Here, we showed that overexpression of Hsp105α alone suppressed the aggregation of truncated AR containing an expanded polyglutamine tract similarly to Hsp70 or Hsp40, whereas Hsp70 and Hsp40 in combination suppressed the aggregation much more markedly. However, because the suppression of aggregation by Hsp70 and Hsp40 was not enhanced by the coexpression of Hsp105α, Hsp105α and Hsp70/Hsp40 seem to suppress the polyglutamine-induced neurotoxicity by similar mechanisms.

In polyglutamine diseases such as spinocerebellar ataxia type 3/Machado-Joseph disease, Hsp70 colocalizes in intracellular aggregates, whereas Hsp105α is not found in the aggregates (27). In the present study, Hsp105 was detected in nuclear inclusions in neurons of the spinal anterior horn and scrotal skin epidermal cells of SBMA patients and also in neurons of the spinal anterior horn and muscle cells of SBMA transgenic mice, although only a few Hsp105-immunoreactive nuclear inclusions were observed in neurons of the spinal cord of the patients and mice. On the other hand, in a cellular model of SBMA, endogenous Hsp70 but not endogenous Hsp105α localized to aggregates of tAR97, although the overexpressed Hsp105α localized to the aggregates of tAR97. Because Hsp70 exists in much larger amounts than Hsp105α in cells, Hsp70 may interact preferentially with truncated AR containing an expanded polyglutamine tract. However, when Hsp105α was overexpressed in the cells, reaching high levels, it seemed to bind and localize to truncated AR containing an expanded polyglutamine tract like Hsp70. Thus, the existence of molecular chaperones at high concentrations in cells may be essential to prevent the aggregation of truncated AR containing an expanded polyglutamine tract.

The intranuclear aggregation of truncated AR containing an expanded polyglutamine tract and apoptotic cell death coincided in the cellular model of SBMA, and both processes were suppressed by overexpression of Hsp105α. As to the mechanism by which Hsp105α suppresses the apoptosis caused by expansion of the polyglutamine tract, one possibility is that suppression of aggregation by Hsp105α mediates suppression of apoptosis. Key components of the transcription apparatus, such as cAMP response element binding protein-binding protein, p53, and $TAF_{II}130$, are sequestered in polyglutamine-containing inclusions, then the expanded polyglutamine tract causes altered gene transcription (30, 53–57). By preventing the formation of intranuclear aggregates, Hsp105α may suppress the alteration of gene transcription caused by an expanded polyglutamine tract and eventually apoptotic cell death.

Another possibility is that the abilities of Hsp105α to suppress aggregate formation and cellular toxicity caused by expansion of the polyglutamine tract are independent. Recently, molecular chaperones, such as Hsp70, Hsp40, and Hsp27, were shown to suppress an expanded polyglutamine-mediated cellular toxicity independently of suppression of aggregation (35, 36). Although the relationship between the aggregation and the induction of apoptosis remains unknown, the suppression of cellular toxicity by molecular chaperones may be caused by the ability to inhibit apoptosis. Hsp105α suppresses heat shock-induced apoptosis in neuronal cells by preventing the activation of c-Jun N-terminal kinase (44). Because c-Jun N-terminal kinase is activated by the expanded polyglutamine tract (58), Hsp105α may also suppress the cellular toxicity by its ability to inhibit apoptosis.

In conclusion, we identified Hsp105α as a novel molecule that reduces aggregation and cellular toxicity caused by an expansion of the polyglutamine tract. Molecular chaperones, such as Hsp105α, Hsp70, Hsp40, and Hsp27, seem to suppress cell toxicity caused by an expansion of the polyglutamine tract. These findings suggest that increasing the expression levels or enhancing the function of chaperones in neurons may open up a promising approach to the treatment of polyglutamine diseases, although more studies are required to determine the precise mechanism of neurodegeneration of CAG repeat diseases.

REFERENCES

1. Kennedy, W. R., Alter, M., and Sung, J. H. (1968) *Neurology* **18**, 671–680
2. Sobue G., Hashizume, Y., Mukai, E., Hirayama, M., Mitsuma, T., and Takahashi, A. (1989) *Brain* **112**, 209–232
3. La Spada, A. R., Wilson, E. M., Lubahn, D. B., Harding, A. E., and Fischbeck, K. H. (1991) *Nature* **352**, 77–79
4. Li, M., Miwa, S., Kobayashi, Y., Merry, D. E., Yamamoto, M., Tanaka, F., Doyu, M., Hashizume, Y., Fischbeck, K. H., and Sobue, G. (1998) *Ann. Neurol.* **44**, 249–254
5. Li, M., Nakagomi, Y., Kobayashi, Y., Merry, D. E., Tanaka, F., Doyu, M., Mitsuma, T., Hashizume, Y., Fischbeck, K. H., and Sobue, G. (1998) *Am. J. Pathol.* **153**, 695–701
6. The Huntington's Disease Collaborative Research Group (1993) *Cell* **72**, 971–983
7. Koide, R., Ikeuchi, T., Onodera, O., Tanaka, H., Igarashi, S., Endo, K., Takahashi, H., Kondo, R., Ishikawa, A., Hayashi, T., Saito, M., Tomoda, A., Miike, T., Naito, H., Ikuta, F., and Tsuji, S. (1994) *Nat. Genet.* **6**, 9–13
8. Nagafuchi, S., Yanagisawa, H., Sato, K., Shirayama, T., Ohsaki, E., Bundo, M., Takeda, T., Tadokoro, K., Kondo, I., Murayama, N., Tanaka, Y., Kikushima, H., Umino, K., Kurosawa, H., Furukawa, T., Nihei, K., Inoue, T., Sano, A., Komura, O., Takahashi, M., Yoshizawa, T., Kanazawa, I., and Yamada, M. (1994) *Nat. Genet.* **6**, 14–18
9. Kawaguchi, Y., Okamoto, T., Taniwaki, M., Aizawa, M., Inoue, M., Katayama, S., Kawamaki, H., Nakamura, S., Nishimura, M., Akiguchi, I., Kimura, J., Narumiya, S., and Kakizuka, A. (1994) *Nat. Genet.* **8**, 221–228
10. Orr, H. T., Chung, M. Y., Banfi, S., Kwiatkowski, T. J., Servadio, A., Beaudet, A. L., McCall, A. E., Duvick, L. A., Ranum, L. P., and Zoghbi, H. Y. (1993) *Nat. Genet.* **4**, 221–226
11. Pulst, S. M., Nechiporuk, A., Nechiporuk, T., Gispert, S., Chen, X. N., Lopes-Cendes, I., Pearlman, S., Starkman, S., Orozco-Diaz, G., Lunkes, A., DeJong, P., Rouleau, G. A., Auburger, G., Korenberg, J. R., Figueroa, C., and Sahba, S. (1996) *Nat. Genet.* **14**, 269–276
12. Sanpei, K., Takano, H., Igarashi, S., Sato, T., Oyake, M., Sasaki, H., Wakisaka, A., Tashiro, K., Ishida, Y., Ikeuchi, T., Koide, R., Saito, M., Sato, A., Tanaka, T., Hanyu, S., Takiyama, Y., Nishizawa, M., Shimizu, N., Nomura, Y., Segawa, M., Iwabuchi, K., Eguchi, I., Tanaka, H., Takahashi, H., and Tsuji, S. (1996) *Nat. Genet.* **14**, 277–284
13. Imbert, G., Saudou, F., Yvert, G., Devys, D., Trottier, Y., Garnier, J. M., Weber, C., Mandel, J. L., Cancel, G., Abbas, N., Durr, A., Didierjean, O., Stevanin, G., Agid, Y., and Brice, A. (1996) *Nat. Genet.* **14**, 285–291

14. Zhuchenko, O., Bailey, J., Bonnen, P., Ashizawa, T., Stockton, D. W., Amos, C., Dobyns, W. B., Subramony, S. H., Zoghbi, H. Y., and Lee, C. C. (1997) *Nat. Genet.* **15**, 62–69
15. David, G., Abbas, N., Stevanin, G., Durr, A., Yvert, G., Cancel, G., Weber, C., Imbert, G., Saudou, F., Antoniou, E., Drabkin, H., Gemmill, R., Giunti, P., Benomar, A., Wood, N., Ruberg, M., Agid, Y., Mandel, J. L., and Brice, A. (1997) *Nat. Genet.* **17**, 65–70
16. Welch, W. J., and Gambetti, P. (1998) *Nature* **392**, 23–24
17. Sherman, M. Y., and Goldberg, A. L. (2001) *Neuron* **29**, 15–32
18. Johnston, J. A., Ward, C. L., and Kopito, R. R. (1998) *J. Cell Biol.* **143**, 1883–1898
19. Schulz, J. B., and Dichgans, J. (1999) *Curr. Opin. Neurol.* **12**, 433–439
20. Heiser, V., Scherzinger, E., Boeddrich, A., Nordhoff, E., Lurz, R., Schugardt, N., Lehrach, H., and Wanker, E. E. (2000) *Proc. Natl. Acad. Sci. U. S. A.* **97**, 6739–6744
21. Kazemi-Esfarjani, P., and Benzer, S. (2000) *Science* **287**, 1837–1840
22. Nagai, Y., Tucker, T., Ren, H., Kenan, D. J., Henderson, B. S., Keene, J. D., Strittmatter, W. J., and Burke, J. R. (2000) *J. Biol. Chem.* **275**, 10437–10442
23. Hendricks, J. P., and Hartl, F. U. (1993) *Annu. Rev. Biochem.* **62**, 349–384
24. Hartl, F. U. (1996) *Nature* **381**, 571–580
25. Muchowski, P. J., Schaffar, G., Sittler, A., Wanker, E. E., Hayer-Hartl, M. K., and Hartl, F. U. (2000) *Proc. Natl. Acad. Sci. U. S. A.* **97**, 7841–7846
26. Cummings, C. J., Mancini, M. A., Antalffy, B., DeFranco, D. B., Orr, H. T., and Zoghbi, H. Y. (1998) *Nat. Genet.* **19**, 148–154
27. Chai, Y., Koppenhafer, S. L., Bonini, N. M., and Paulson, H. L. (1999) *J. Neurosci.* **19**, 10338–10347
28. Jana, N. R., Tanaka, M., Wang, G., and Nukina, N. (2000) *Hum. Mol. Genet.* **9**, 2009–2018
29. Kobayashi, Y., Kume, A., Li, M., Doyu, M., Hata, M., Ohtsuka, K., and Sobue, G. (2000) *J. Biol. Chem.* **275**, 8772–8778
30. Stenoien, D. L., Cummings, C. J., Adams, H. P., Mancini, M. G., Patel, K., DeMartino, G. N., Marcelli, M., Weigel, N. L., and Mancini, M. A. (1999) *Hum. Mol. Genet.* **8**, 731–741
31. Wyttenbach, A., Carmichael, J., Swartz, J., Furlong, R. A., Narain, Y., Rankin, J., and Rubinsztein, D. C. (2000) *Proc. Natl. Acad. Sci. U. S. A.* **97**, 2898–2903
32. Warrick, J. M., Chan, H. Y., Gray-Board, G. L., Chai, Y., Paulson, H. L., and Bonini, N. M. (1999) *Nat. Genet.* **23**, 425–428
33. Cummings, C. J., Sun, Y., Opal, P., Antalffy, B., Mestril, R., Orr, H. T., Dillmann, W. H., and Zoghbi, H. Y. (2001) *Hum. Mol. Genet.* **10**, 1511–1518
34. Adachi, H., Katsuno, M., Minamiyama, M., Sang, C., Pagoulatos, G., Angelidis, C., Kusakabe, M., Yoshiki, A., Kobayashi, Y., Doyu, M., and Sobue, G. (2003) *J. Neurosci.* **23**, 2203–2211
35. Wyttenbach, A., Sauvageot, O., Carmichael, J., Diaz-Latoud, C., Arrigo, A. P., and Rubinsztein, D. C. (2002) *Hum. Mol. Genet.* **11**, 1137–1151
36. Zhou, H., Li, S. H., and Li, X. J. (2001) *J. Biol. Chem.* **276**, 48417–48424
37. Ishihara, K., Yasuda, K., and Hatayama, T. (1999) *Biochim. Biophys. Acta* **1444**, 138–142
38. Yasuda, K., Nakai, A., Hatayama, T., and Nagata, K. (1995) *J. Biol. Chem.* **270**, 29718–29723
39. Lee-Yoon, D., Easton, D., Murawski, M., Burd, R., and Subjeck, J. R. (1995) *J. Biol. Chem.* **270**, 15725–15733
40. Plesofsky-Vig, N., and Brambl, R. (1998) *J. Biol. Chem.* **273**, 11335–11341
41. Storozhenko, S., De Pauw, P., Kushnir, S., Van Montagu, M., and Inze, D. (1996) *FEBS Lett.* **390**, 113–118
42. Mukai, H., Kuno, T., Tanaka, H., Hirata, D., Miyakawa, T., and Tanaka, C. (1993) *Gene (Amst.)* **132**, 57–66
43. Wakatsuki, T., and Hatayama, T. (1998) *Biol. Pharm. Bull.* **21**, 905–910
44. Hatayama, T., Yamagishi, N., Minobe, E., and Sakai, K. (2001) *Biochem. Biophys. Res. Commun.* **288**, 528–534
45. Yamagishi, N., Nishihori, H., Ishihara, K., Ohtsuka, K., and Hatayama, T., (2000) *Biochem. Biophys. Res. Commun.* **272**, 850–855
46. Michels, A. A., Kanon, B., Konings, A. W. T., Ohtsuka, K., Bensaude, O., and Kampinga, H. H. (1997) *J. Biol. Chem.* **272**, 33283–33289
47. Merry, D. E., Kobayashi, Y., Bailey, C. K., Taye, A. A., and Fischbeck, K. H. (1998) *Hum. Mol. Genet.* **7**, 693–701
48. Honda, K., Hatayama, T., and Yukioka, M. (1989) *Biochem. Biophys. Res. Commun.* **160**, 60–66
49. Katsuno, M., Adachi, H., Kume, A., Li, M., Nakagomi, Y., Niwa, H., Sang, C., Kobayashi, Y., Doyu, M., and Sobue, G. (2002) *Neuron* **35**, 843–854
50. Rüdiger, S., Buchberger A., and Bukau, B. (1997) *Nat. Struct. Biol.* **4**, 342–349
51. Bukau, B., and Horwich, A. L. (1998) *Cell* **92**, 351–366
52. Freeman, B. C., Myers, M. P., Schumacher, R., and Morimoto, R. I. (1995) *EMBO J.* **14**, 2281–2292
53. McCampbell, A., Taylor, J. P., Taye, A. A., Robitschek, J., Li, M., Walcott, J., Merry, D., Chai, Y., Paulson, H., Sobue, G., and Fischbeck, K. H. (2000) *Hum. Mol. Genet.* **9**, 2197–2202
54. Staffan, J. S., Kazantsev, A., Spasic-Boskovic, O., Greenwald, M., Zhu, Y. Z., Gohler, H., Wanker, E. E., Bates, G. P., Housman, D. E., and Thompson, L. M. (2000) *Proc. Natl. Acad. Sci. U. S. A.* **97**, 6763–6768
55. Kazantsev, A., Preisinger, E., Dranovsky, A., Goldgaber, D., and Housman, D. (1999) *Proc. Natl. Acad. Sci. U. S. A.* **96**, 11404–11409
56. Boutell, J. M., Thomas, P., Neal, J. W., Weston, V. J., Duce, J., Harper, P. S., and Jones, A. L. (1999) *Hum. Mol. Genet.* **8**, 1647–1655
57. Shimohata, T., Nakajima, T., Yamada, M., Uchida, C., Onodera, O., Naruse, S., Kimura, T., Koide, R., Nozaki, K., Sano, Y., Ishiguro, H., Sakoe, K., Ooshima, T., Sato, A., Ikeuchi, T., Oyake, M., Sato, T., Aoyagi, Y., Hozumi, I., Nagatsu, T., Takiyama, Y., Nishizawa, M., Goto, J., Kanazawa, I., Davidson, I., Tanese, N., Takahashi, H., and Tsuji, S. (2000) *Nat. Genet.* **26**, 29–36
58. Yasuda, S., Inoue, K., Hirabayashi, M., Higashiyama, H., Yamamoto, Y., Fuyuhiro, H., Komure, O., Tanaka, F., Sobue, G., Tsuchiya, K., Hamada, K., Sasaki, H., Takeda, K., Ichijo, H., and Kakizuka, A. (1999) *Genes Cells* **4**, 743–756

American Journal of Pathology, Vol. 163, No. 2, August 2003

Dorfin Localizes to the Ubiquitylated Inclusions in Parkinson's Disease, Dementia with Lewy Bodies, Multiple System Atrophy, and Amyotrophic Lateral Sclerosis

Nozomi Hishikawa,* Jun-ichi Niwa,* Manabu Doyu,* Takashi Ito,* Shinsuke Ishigaki,* Yoshio Hashizume,† and Gen Sobue*

From the Department of Neurology, Nagoya University Graduate School of Medicine, Nagoya; and the Department of Neuropathology,† Institute for Medical Sciences of Aging, Aichi Medical University, Aichi, Japan*

In many neurodegenerative diseases, the cytopathological hallmark is the presence of ubiquitylated inclusions consisting of insoluble protein aggregates. Lewy bodies in Parkinson's disease and dementia with Lewy bodies disease, glial cell inclusions in multiple system atrophy, and hyaline inclusions in amyotrophic lateral sclerosis (ALS) are representative of these inclusions. The elucidation of the components of these inclusions and the mechanisms underlying inclusion formation is important in uncovering the pathogenesis of these disorders. We hypothesized that Dorfin, a perinuclearly located E3 ubiquitin ligase, participates in the formation of ubiquitylated inclusions in a wide range of neurodegenerative diseases. Here, we report that affinity-purified anti-Dorfin antibody labeled ubiquitylated inclusions of Parkinson's disease, dementia with Lewy bodies disease, multiple system atrophy, and sporadic and familial ALS. A double-immunofluorescence study revealed that Dorfin shows a distribution pattern parallel to that of ubiquitin. Furthermore, by a filter trap assay, we detected that Dorfin is present in the ubiquitylated high-molecular weight structures derived from these diseases. These results suggest that Dorfin plays a crucial role in the formation of ubiquitylated inclusions of α-synucleinopathy and ALS. However, because we failed to show the direct binding of α-synuclein with Dorfin, future investigations into the binding partner(s) of Dorfin will be needed to deepen our understanding of the pathophysiology of α-synucleinopathy and ALS. *(Am J Pathol 2003, 163:609–619)*

Protein aggregates are formed when the cell fails to further degrade misfolded or mutated proteins. Protein aggregates are generally difficult to unfold or degrade; their formation in cells is related to the pathogenesis of several common aging-related neurodegenerative diseases including Parkinson's disease (PD), amyotrophic lateral sclerosis (ALS), polyglutamine disease (Huntington's disease and spinocerebellar ataxias resulting from an expanded CAG repeat in their causative gene), and Alzheimer's disease.[1,2] These group of disorders are called conformational diseases, in which the underlying protein aggregation results from β-sheet linkages.[1] Furthermore, the characteristic intracellular inclusions composed of aggregated ubiquitylated protein surrounded by disorganized filaments are the common histopathological hallmark of many neurodegenerative diseases.[3] Lewy bodies (LBs) in PD and dementia with Lewy bodies (DLB), glial cell inclusions (GCIs) in multiple system atrophy (MSA), and hyaline and skein-like inclusions in ALS are representative of such inclusions.[4–8] To elucidate the mechanisms underlying inclusion body formation and neurodegeneration, it is important to know which protein components are involved.

We have reported previously that Dorfin is predominantly localized in neuronal hyaline inclusions found in familial ALS with *SOD1* mutation and in *SOD1*^{G93A}-transgenic mice.[9] Dorfin is a gene product we cloned from the anterior horn tissues of the human spinal cord.[10] Its mRNA is ubiquitously expressed through the central nervous system, including the spinal cord. Dorfin contains a RING-finger/IBR (in-between ring-finger) domain[11–13] at its N-terminus and mediates E3 ubiquitin (Ub) ligase activity.[10] Dorfin physically binds and ubiquitylates various SOD1 mutants derived from familial ALS patients and enhances their degradation, but it has no effect on the stability of wild-type SOD1.[9] Overexpression of Dorfin protects neural cells against the toxic effects of mutant SOD1 and reduces SOD1 inclusions.[9] Our previous results indicate that Dorfin protects neurons by recognizing

Supported by grants from the Ministry of Education, Culture, Sports, Science, and Technology, and from the Ministry of Health, Labor, and Welfare of Japan.

Accepted for publication April 24, 2003.

Address reprint requests to Gen Sobue, M.D., Ph.D., Department of Neurology, Nagoya University Graduate School of Medicine, Tsurumai, Nagoya 466-8550, Japan. E-mail: sobueg@med.nagoya-u.ac.jp.

and then ubiquitylating mutant SOD1 proteins, subsequently targeting them for proteasomal degradation.

Mutant SOD1 protein is fairly unstable compared to its wild-type, and toxic gain of function is thought to be related to this unstable conformation.[14,15] Recently, CHIP (carboxyl terminus of Hsc70-interacting protein), U-box type E3, has been shown to interact with Hsp90 or Hsp70 and to ubiquitylate unfolded proteins trapped by these molecular chaperones, thus acting as a quality control E3.[16–18] The physiological role of Dorfin remains unknown, but it may be regarded as another quality control E3 because it can discriminate between the normal and abnormal status of SOD1 proteins.[9] In cultured cells, Dorfin resides in the perinuclear region and forms aggresome-like structures.[10] Aggresomes are perinuclear cytoplasmic inclusions containing misfolded ubiquitylated proteins that appear when the cell fails to further degrade such proteins.[19,20] Thus, an important and interesting question in this context is whether Dorfin plays a role in neurodegenerative diseases with cytosolic ubiquitylated inclusions other than familial ALS with SOD1 mutations through ubiquitylation of target proteins. To address this question, using immunohistochemical analysis of Dorfin, we examined various neurodegenerative diseases with ubiquitylated inclusion bodies, including α-synucleinopathy (sporadic PD, DLB, and MSA) as well as motor neuron disease (sporadic and familial ALS). We here report that Dorfin co-localizes to the ubiquitylated inclusion bodies in these neurodegenerative diseases, and we suggest that Dorfin plays an important role in the disease process.

Materials and Methods

Tissue Samples

The participants of this study were five PD patients (age, 67 to 79 years; four men and one women), five cases of DLB (age, 65 to 78 years; four men and one women), five with MSA (age, 60 to 72 years; three men and two women), two men with sporadic ALS (SALS) (age, 68 and 69 years), one man with familial ALS (FALS) (57 years), and five controls without neurological disease (C; age, 61 to 78 years; four men and one women). Diagnoses of all cases were confirmed by clinical and pathological diagnostic criteria for each disease.[21–23] The brain and spinal cord were removed at autopsy performed 4 to 12 hours postmortem. The midbrain for PD, cerebral cortex of the temporal lobe for DLB, putamen and midbrain for MSA, and the spinal cords for SALS and FALS were excised and subjected to extensive study for each disease. These tissues were fixed in 20% buffered formalin and embedded in paraffin.

Characterization of Anti-Dorfin Antibody

Polyclonal rabbit antiserum (Dorfin-30) was raised against a C-terminal portion (amino acids 678 to 690) of Dorfin as described.[10] A synthetic peptide, RKIHNRYEGKDVSKHKRN (corresponding to amino acid sequence of residues 396 to 413 of Dorfin), was used for immunization in rabbit and affinity-purified to raise another polyclonal antiserum against Dorfin (Dorfin-41). Brain (cerebral cortex and putamen) and spinal cord tissues from normal controls without neurological disease were homogenized in sodium dodecyl sulfate (SDS) lysis buffer (10 mmol/L Tris, pH 8.0, 150 mmol/L NaCl, 2% SDS) with a protease inhibitor mixture (Complete; Roche Diagnostics, Basel, Switzerland) and were fractionated by centrifugation at 16,000 × *g*. The protein concentration was determined with a DC protein assay kit (Bio-Rad, Hercules, CA), and supernatants were used for Western blotting analysis. Construction of an N-terminal Xpress-tagged Dorfin expression vector (pcDNA4/HisMax-Dorfin) and Myc-tagged Ub expression vector (pcDNA3.1Myc-Ub) was reported elsewhere.[10] A C-terminal Myc-tagged Dorfin expression vector was constructed from cDNA containing the entire coding region of Dorfin inserted in-frame into the *Kpn*I and *Xba*I site of pcDNA3.1/MycHis(+) vector (Invitrogen, Carlsbad, CA). A N-terminal FLAG-tagged Dorfin expression vector was constructed from cDNA containing the entire coding region of Dorfin inserted in-frame into the *Cla*I and *Kpn*I site of pFLAG-CMV-2 vector (Sigma, St. Louis, MO). pcDNA3.1(+)FLAG-CHIP and pcDNA3.1(+)FLAG-parkin were kind gifts from Dr. Keiji Tanaka (Tokyo Metropolitan Institute of Medical Science) and Dr. Nobutaka Hattori (Juntendo University School of Medicine), respectively. Human embryonic kidney 293 (HEK293) cells were maintained in Dulbecco's modified Eagle's medium with 10% fetal calf serum. Transfections were performed using the Effectene transfection reagent (Qiagen, Hilden, Germany). Cells were cultured for 24 hours and lysed in TNES lysis buffer (50 mmol/L Tris, 150 mmol/L NaCl, 1% Nonidet P-40, and 0.1% SDS) with a protease inhibitor mixture (Roche Diagnostics). The protein concentration was determined with a DC protein assay kit (Bio-Rad), and lysates were electrophoresed by SDS-polyacrylamide gel electrophoresis and transferred to Hybond-P polyvinylidene difluoride membrane (Amersham Pharmacia, Piscataway, NJ) for Western blotting. The membranes were blocked in 5% milk in Tris-buffered saline (TBS) containing 0.1% Tween-20, and incubated overnight at 4°C with Dorfin antiserum (1:5000 dilution). The blots were then washed three times for 10 minutes each in TBS with 0.1% Tween 20, followed by a 1-hour incubation in horseradish peroxidase coupled to secondary antibody (1:5000 dilution, Amersham Pharmacia). The blots were then washed three times for 10 minutes each in TBS with 0.1% Tween 20 before incubation in enhanced chemiluminescence reagent (Amersham Pharmacia) and exposure to film.

Immunohistochemistry and Immunoelectron Microscopy

Immunohistochemistry was performed as described previously.[24–26] Four-μm-thick sections were obtained from the paraffin-embedded midbrain, cerebral cortex, putamen, hippocampus, and spinal cord of the patients with PD, DLB, MSA, SALS, FALS, and controls, respectively. These sections were immunostained using the avidin-

biotin-peroxidase complex method with 3.3-diaminobenzidine tetrahydrochloride (Wako, Osaka, Japan) as a chromogen. The immunolabeled sections were lightly counterstained with hematoxylin. Dorfin antiserum (1:200 dilution in both Dorfin-30 and Dorfin-41), and anti-Ub (P4D1, 1: 400 dilution; Santa Cruz Biotechnology, Santa Cruz, CA) antibodies were used. For staining with anti-Dorfin antiserum, the sections were pretreated with 99% formic acid (Wako) for 5 minutes at room temperature. Specificity of anti-Dorfin antibody on immunostaining for human tissue was assessed by the preabsorption of antibody with peptide antigen. To assess the co-localization of Dorfin and Ub, a double-labeling immunofluorescence study was performed on the selected sections with a combination of anti-Dorfin and anti-Ub antibodies. Anti-Dorfin antibody was visualized by anti-rabbit goat IgG coupled with Alexa Fluor 568 (Molecular Probes, Eugene, OR), and anti-Ub antibody was visualized with anti-mouse sheep IgG coupled with Alexa Fluor 488 (Molecular Probes), and observed under a LSM-510 confocal microscope (Carl Zeiss, Gottingen, Germany). To assess Dorfin immunoreactivity in ubiquitylated inclusions, serial sections were prepared for every two serial sections; one was stained with anti-Dorfin antibody and the other with anti-Ub antibody. The ratio of Dorfin-positive inclusion bodies among Ub-positive inclusions was evaluated by assessing 40 to 120 Ub-positive inclusion bodies in each case of PD, DLB, MSA, and at least 10 inclusion bodies in FALS and SALS.

Immunoelectron microscopy was performed as previously described.[24,25] The selected deparaffinized sections were immunostained with Dorfin-30 antibody in the same manner, then washed in phosphate buffer, post-fixed with 1% osmium tetroxide, dehydrated in a graded series of ethanol, and embedded in epoxy resin. Ultrathin sections were prepared and examined under an H-7000 electron microscope (Hitachi, Tokyo, Japan). Each immunohistochemical reaction was ascertained by substituting normal rabbit or mouse sera for the primary antibodies, and no specific peroxidase reactions occurred in these control experiments.

Filter Trap Assay

For this assay, ~100- to 200-mg tissues from the cerebral cortex of DLB, putamen of MSA, and the cerebral cortex and spinal cord of ALS and control were used. A filter trap assay was performed as previously described.[27] Tissues were homogenized in 10 vol of TBS. Homogenates were centrifuged at 800 × *g* for 10 minutes at 4°C and the supernatants were diluted with 10 vol of TBS with 0.1% SDS. Protein concentrations were determined with a DC protein assay kit (Bio-Rad) and, using a slot blot device (Bio-Rad), the supernatants were filtered under vacuum through 0.22-μm cellulose acetate membranes (Sartorius, Gottingen, Germany) followed by two washes in TBS. The membranes were then incubated in 5% dry milk in TBS at room temperature for 1 hour, followed by an overnight incubation at 4°C with Dorfin-30 (1:5000 dilution), anti-Ub (1:1000 dilution; Zymed, San Francisco, CA) or anti-α-synuclein (LB509, 1:1000 dilution; Zymed) antibody in TBS with 0.1% Tween 20. Horseradish peroxidase-conjugated second antibodies (1:5000, Amersham Pharmacia) were used and detected with enhanced chemiluminescence reagent (Amersham Pharmacia). To confirm equal loading of proteins, the same samples were filter trapped using 0.45-μm nitrocellulose membranes (Bio-Rad) and were probed with anti-α-tubulin antibody (1:1000 dilution, Sigma).

Fractionation of Normal and Diseased Brain Tissues

Approximately 100- to 200-mg tissues of cingulate gyrus from normal or DLB brains, 200-mg tissues of putamen from MSA brains, or 400-mg ALS spinal cord were homogenized in 10 vol of lysis buffer A (50 mmol/L Tris-HCl at pH 7.5, 500 mmol/L NaCl, 5 mmol/L ethylenediaminetetraacetic acid, and 10 mmol/L NaF) with a protease inhibitor mixture (Complete, Roche Diagnostics) and centrifuged at 16,000 × *g* for 30 minutes at 4°C. Resulting pellets were sequentially extracted by homogenization in Triton X-100 (buffer A containing 1% Triton X-100), and urea (50 mmol/L Tris-HCl, 8 mol/L urea, 1 mmol/L EGTA) followed by centrifugation at 100,000 × *g*.

Immunoprecipitation

α-Synuclein cDNA was amplified by polymerase chain reaction from human brain cDNAs and cloned into the *Eco*RV site of pcDNA3.1/MycHis(+) (Invitrogen). To generate the mutant α-synuclein expression vector, A30P and A53T mutations were introduced into the pcDNA3.1/MycHis-α-synuclein with a QuickChange site-directed mutagenesis Kit (Stratagene, La Jolla, CA) according to Lee and colleagues.[28] Construction of pcDNA3.1/MycHis-wild-type and G85R mutant SOD1 vector was previously described.[9] Xpress-tagged Dorfin (pcDNA4/HisMax-Dorfin) and Myc-tagged α-synuclein or SOD1 were transiently expressed using the Effectene transfection reagent (Qiagen) in HEK293 cells. Cells were lysed in TNES lysis buffer with a protease inhibitor mixture (Roche Diagnostics). To inhibit cellular proteasome activity, cells were treated with 0.5 μmol/L MG132 (Z-Leu-Leu-Leu-al; Sigma) for 16 hours after overnight posttransfection. Immunoprecipitation from the transfected cell lysates was performed with 2 μg of anti-Xpress antibody (Invitrogen) and protein A/G Plus agarose (Santa Cruz Biotechnology), and then washed four times in lysis buffer. Immunoprecipitates were analyzed by Western blotting with enhanced chemiluminescence detection reagents (Amersham Pharmacia).

Results

Specificity of Anti-Dorfin Antibody

To examine the pathophysiological role of Dorfin, we raised affinity-purified antisera to two separate regions of human Dorfin (Figure 1A) and characterized their speci-

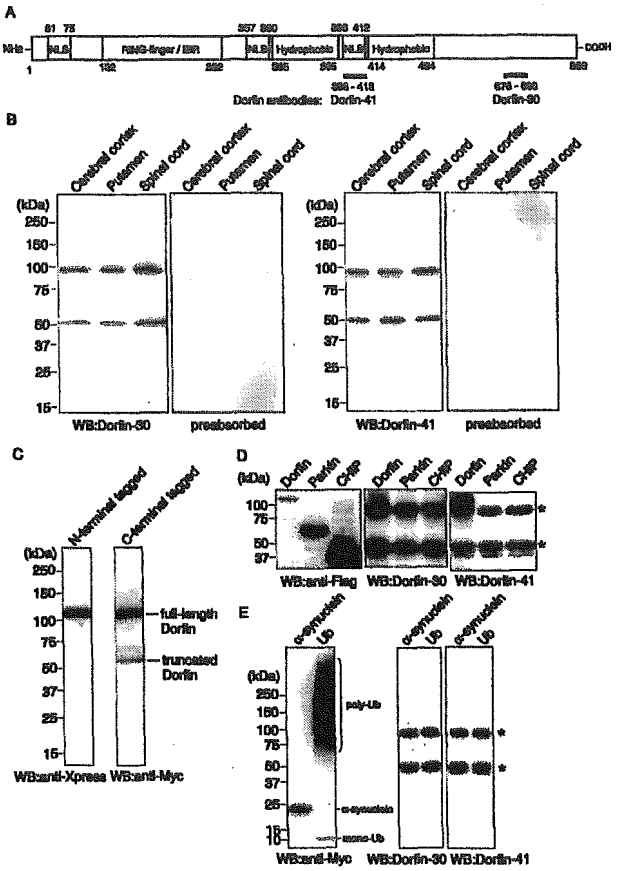

Figure 1. Characterization of affinity-purified antibody to human Dorfin. **A:** Schematic diagram of human Dorfin and peptide antibodies. IBR, in-between ring-finger; NLS, nuclear localization signal-like sequence. **B:** SDS-polyacrylamide gel electrophoresis and Western blotting analysis of the extracted protein from human central nervous tissues. Soluble extracts from normal adult brains (cerebral cortex and putamen) and spinal cord (50 μg each) were used and probed with antibodies to Dorfin. Note that antiserum preabsorbed with excess peptide antigen shows no staining. **C:** SDS-polyacrylamide gel electrophoresis and Western blotting analysis of lysates of HEK293 cells expressing Xpress-Dorfin (**left**) or Dorfin-Myc (**right**). Note that only C-terminal Myc-tagged Dorfin shows truncated fragment. **D:** Specific binding of anti-Dorfin antibodies to Dorfin proteins. Lysates of HEK293 cells expressing FLAG-tagged Dorfin, parkin, and CHIP were analyzed by Western blotting with antibodies to Dorfin. Both Dorfin-30 and Dorfin-41 recognize only Dorfin fusion proteins. **E:** Anti-Dorfin antibodies do not cross-react with α-synuclein and Ub. Lysates of HEK293 cells expressing Myc-tagged α-synuclein and Ub were analyzed by Western blotting with antibodies to Dorfin. Both Dorfin-30 and Dorfin-41 recognize only endogenous Dorfin. **Asterisks** on the **right** indicate endogenous Dorfin.

ficity. First, we tested Dorfin antisera by Western blotting under reduced conditions against brain and spinal cord tissues from a control subject without neurological disease. In this assay, both Dorfin-30 (amino acids 678 to 690) and Dorfin-41 (amino acids 396 to 413) recognized these tissues' cognate antigens in a specific manner, and recognized ~98-kd and ~52-kd protein of human brain extracts as well as those of spinal cord extracts (Figure 1B, left). Their reactivities were abolished by preabsorption with the excess of peptide antigens (Figure 1B, right). The ~98-kd protein probably corresponds to the full-length Dorfin protein because the calculated molecular weight of Dorfin is ~91 kd. The ~52-kd band is thought to be a truncated C-terminal fragment of Dorfin recognized by Dorfin antiserum. To confirm this inference, we next examined the size of N-terminal Xpress-tagged and C-terminal Myc-tagged Dorfin fusion proteins expressed in the cultured cell line HEK293 by Western blotting. Both anti-Xpress and anti-Myc antibody recognized ~102-kd full-length proteins, but only anti-Myc antibody to the C-terminal tag revealed the ~60-kd truncated C-terminal fragment (Figure 1C). Similar results have been reported by another laboratory, using various mouse tissues with anti-XYbp antiserum (*XYbp* is a mouse orthologue of *Dorfin*) in Western blotting analysis.[29] Furthermore, we determined the selective specificity of our antibodies to Dorfin. We assessed whether our antibodies recognize other E3 ligases, although two epitope regions, we have chosen to create anti-Dorfin antibodies, show no homology to other proteins with BLASTp searches in the database of National Center for Biotechnology Information. We chose E3 ligases, parkin, and CHIP as controls, because parkin has RING-finger/IBR domain,[11] localizes in the LBs,[30] and ubiquitylates unfolded protein(s)[31] as well as Dorfin, and CHIP is also E3 ligase for abnormal proteins as the so-called protein quality control ligase[16–18] and interacts with parkin to enhance its activity.[32] N-terminal FLAG-tagged fusion proteins of Dorfin, parkin, and CHIP were examined by Western blotting with Dorfin-30 and Dorfin-41 antibodies. Both anti-Dorfin antibodies recognized ~102-kd full-length fusion proteins and endogenous Dorfin, but did not recognized parkin and CHIP at all (Figure 1D). In addition, we confirmed that anti-Dorfin antibodies do not cross-react with α-synuclein and Ub (Figure 1E).

Dorfin Localizes to Ubiquitylated Inclusion Bodies of PD, DLB, MSA, and ALS

To assess Dorfin immunoreactivity in the involved lesions of the central nervous system of neurodegenerative diseases, we examined the inclusion body-rich regions of the brain and spinal cord sections from sporadic PD, DLB, MSA, sporadic and familial ALS, and normal controls by light and electron microscopic immunohistochemistry.

In PD, both anti-Dorfin antisera, Dorfin-30 and Dorfin-41, labeled LBs of various types existing inside and outside the substantia nigra. More intense immunoreactivity was observed in LBs with Dorfin-41 antibodies. The peripheral rims of typical LBs, either round or elongated, in neuronal cell bodies and in processes were strongly stained, whereas the central cores remained unstained or only weakly stained (Figure 2; A, B, and M). The pale body, Lewy neuritis, axonal spheroids in substantia nigra, and the glial inclusions were also immunostained by both anti-Dorfin antibodies (Figure 2, C and N). Ubiquitin was predominantly seen in rims of LBs, but sometimes in the core of LB. Most, if not all, α-synuclein-positive LBs are also ubiquitin-positive[33] and we have previously shown that Dorfin co-localized with ubiquitylated hyaline inclusions in ALS.[9] Thus, we counted Dorfin-positive inclusions in comparison with ubiquitin. Serial sections stained with anti-Dorfin and anti-Ub antibodies showed that 40.9 ± 12.1% of Ub-positive LBs were positive for Dorfin-30, and 92.2 ± 11.8% of them were positive for Dorfin-41

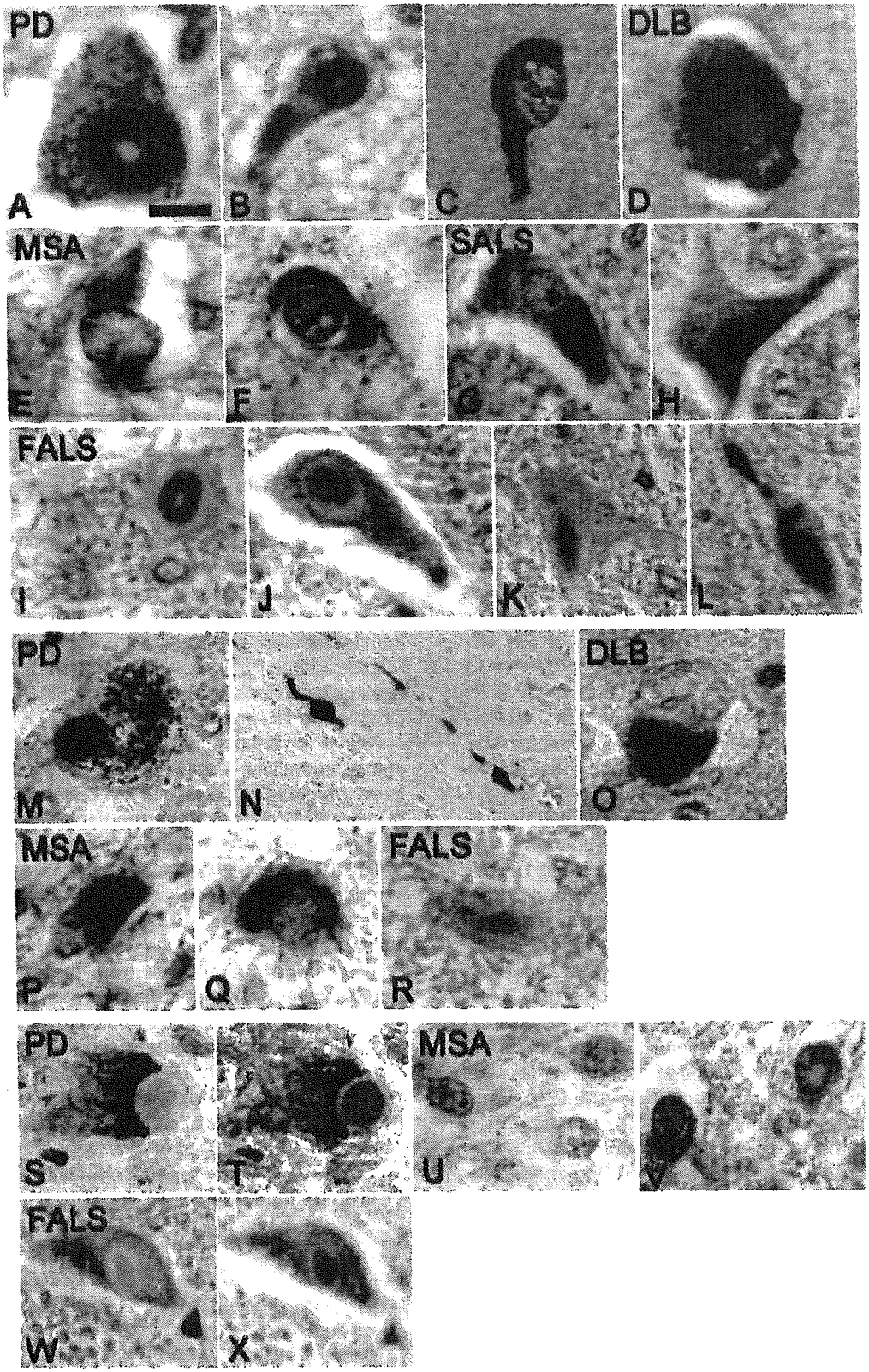

Figure 2. Light microscopic Dorfin immunohistochemistry in neuronal and glial inclusions of PD, DLB, MSA, SALS, and FALS. Immunostainings with Dorfin-30 antibody (**A–L**, **P–X**) and Dorfin-41 antibody (**M–O**) are shown. LBs in the substantial nigral neurons (**A** and **M**) and in the Edinger-Westphal nucleus (**B**) of PD patients are heavily Dorfin-immunoreactive. GCIs (**C**) and Lewy neuritis (**N**) of PD patients are also Dorfin-immunoreactive. Cortical LBs in the temporal cortex of the DLB patient are Dorfin-positive (**D** and **O**). Glial inclusions of the oligodendroglia in MSA patients in the putamen are Dorfin-immunoreactive (**E**, **F**, **P**, and **Q**). Dorfin is also localized in the cytoplasmic inclusions of the spinal motor neurons of SALS patients (**G** and **H**). Dorfin is localized in the LB-like inclusions (**I**, **J**, and **K**) and skein-like inclusions (**K** and **L**) in the remaining motor neurons of the FALS spinal cord. Each inclusion was strongly immunostained by Dorfin (**T**, **V**, and **X**), whereas preabsorbed antibody abolished most immunoreactivity (**S**, **U**, and **W**). **S** and **T**: LBs in pigmented neuron of the substantia nigra in PD. **U** and **V**: GCIs of the putamen in MSA. **W** and **X**: LB-like inclusion of hypoglossal neuron of a FALS case. Scale bar in **A** is equivalent to: 20 μm (**A**, **B**, **G**, **J**, **L**, and **M**); 10 μm (**C**, **D**, **I**, and **O**); 5 μm (**E**, **F**, **P**, and **Q**); 16 μm (**H**, **K**, and **R**), 52 μm (**N**), 12 μm (**S–V**); 8 μm (**W** and **X**).

Table 1. Dorfin and Ubiquitin Immunoreactivity in Neuronal and Glial Inclusions of PD, DLB, MSA, and ALS

Antibody	Dorfin (+) inclusions (assessed number)	Ubiquitin (+) inclusions (assessed number)	Dorfin (+)/ubiquitin (+) (%)
PD (n = 5)			
Dorfin-30	33.8 ± 11.4	68.6 ± 10.5	40.9 ± 12.1
Dorfin-41	52.4 ± 6.5	57.2 ± 4.1	92.2 ± 11.8
DLB (n = 5)			
Dorfin-30	34.2 ± 12.8	53.6 ± 17.8	62.6 ± 13.7
Dorfin-41	52.4 ± 4.3	64.0 ± 8.0	85.4 ± 9.2
MSA (n = 5)			
Dorfin-30	85.0 ± 18.5	125.0 ± 28.9	70.9 ± 20.5
Dorfin-41	69.0 ± 13.5	73.8 ± 9.2	92.9 ± 7.5
SALS (n = 2)			
Dorfin-30	7	17	41.2
Dorfin-41	4	17	23.5
FALS (n = 1)			
Dorfin-30	15	31	48.4
Dorfin-41	14	31	45.2

(+), Immunoreactive.
Numbers of Dorfin- and ubiquitin-immunoreactive inclusions were assessed on 10 consecutive sections. Values are shown as mean ± SD for samples indicated in parentheses.

(Table 1). In DLB, Dorfin-30 and Dorfin-41 labeled the cortical type LB (Figure 2, D and O). Lewy neurites in the hippocampal CA2-3 region and glial inclusions were also immunolabeled by anti-Dorfin antibody as they were in PD (data not shown). The 62.6 ± 13.7% of the Ub-positive cortical LBs were immunoreactive for Dorfin-30, and the 85.4 ± 9.2% of them were immunoreactive for Dorfin-41 (Table 1). In MSA, GCIs observed in the oligodendroglia were immunostained by anti-Dorfin antibody. Dorfin-immunoreactive inclusions appear as flame-shaped (Figure 2, E and P) or sickle-shaped (Figure 2, F and Q) in glial cells. The 70.9 ± 20.5% of ubiquitin-positive GCIs were labeled by Dorfin-30 antibody, and 92.2 ± 11.8% were by Dorfin-41 antibody (Table 1). Only a few of the neuronal cytoplasmic inclusions and neuronal and glial nuclear inclusions were positive for Dorfin (data not shown). In SALS and FALS, eosinophilic, Ub-positive cytoplasmic inclusions and skein-like inclusions were found in motor neurons of the spinal cord.[7] LB-like hyaline inclusions (LBHIs) were also ubiquitylated.[7] Dorfin-30 and Dorfin-41 labeled some of these inclusions, such as the ring-, round-, irregular round-, filamentous rod-, and loose ball-shaped types (Figure 2; G to L and R). Dorfin immunoreactivity was strongly present in the central core of the round- or irregular round-shaped inclusions, and in the middle layer of the ring-shaped inclusions, whereas the outer layers of these inclusions were less immunoreactive (Figure 2; H to J). The Bunina body, which was negative for anti-Ub antibody, was not stained with Dorfin-30 and Dorfin-41 antibody (data not shown). Dorfin-30 was positive at 48.4% of Ub-positive inclusions in SALS and 41.2% in FALS, and Dorfin-41 was positive at 23.5% in SALS and 45.2% in FALS (Table 1). These inclusions were only weakly stained by Dorfin-41. Preabsorbed anti-Dorfin antibody abolished most immunoreactivity (Figure 2; S to X), indicating that our anti-Dorfin antibody specifically recognizes Dorfin-epitopes on the inclusions of these tissues. In normal control, no Dorfin-immunoreactive structure was detected (data not shown).

A double-labeled immunofluorescence study revealed that Dorfin-30 and Ub were co-localized in LBs (Figure 3; A to C). Pale bodies, which have been considered to be the precursors of LB,[34] and Lewy neurites were also immunolabeled by anti-Dorfin and anti-Ub antibodies (Figure 3; D to F). GCIs in MSA (Figure 3; G to I), and the hyaline inclusions in FALS (Figure 3; J to L) were also Dorfin- and Ub-immunoreactive.

At the immunoelectron microscopic level, Dorfin-30 immunoreactivity was localized on filamentous structures, particularly the halo of the LBs that was composed of the radially arranged intermediate filaments associated with granular materials and vesicular structures. These radial filaments and associated structures were strongly immunostained by anti-Dorfin antibody, whereas the central core was not stained (Figure 4, A and B). Thus, the staining profile of Dorfin was very similar to that of Ub and α-synuclein,[33] but different from that of parkin, which localizes predominantly to the core of LBs.[30] Dorfin immunoreactivity in GCI of MSA was composed of randomly arranged tubules or filamentous structures associated with granular materials (Figure 4, C and D). In FALS, the thicker, granule-coated filaments were decorated by the Dorfin immunoreactive deposit and formed the core, whereas the thinner filaments without a granular coating were not recognized by anti-Dorfin antibody and formed the halo (Figure 4, E and F).

Dorfin Accumulation in Ubiquitylated High-Molecular Weight Complexes

In studies of polyglutamine disorders, it has been demonstrated that high-molecular weight aggregates of mutant proteins are retained by filtration through cellulose acetate.[35,36] In a *SOD1*-transgenic mice ALS model, this assay is also applied to detect mutant SOD1 aggregation.[27] Cellulose acetate membranes usually bind protein very poorly and are used to filter high-molecular weight structures from complex mixtures.[35] Thus we investi-

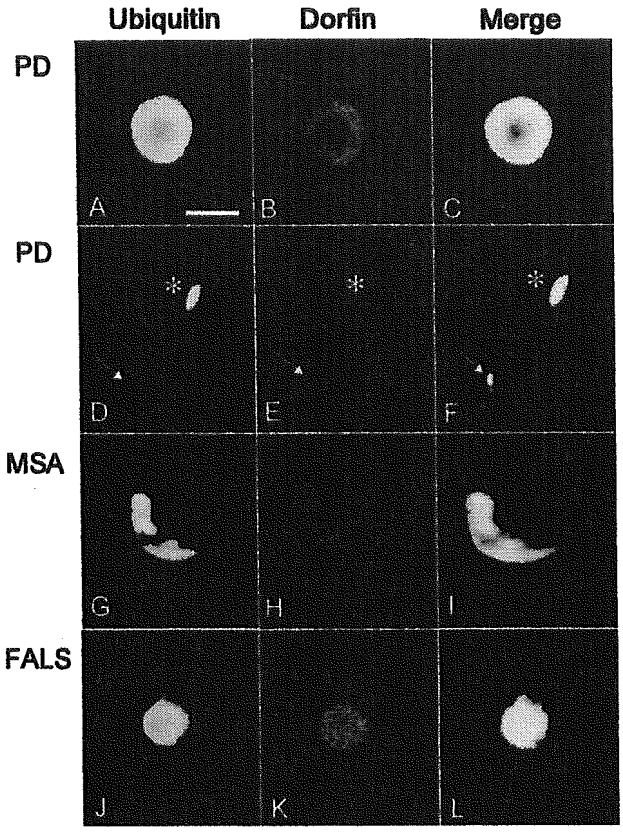

Figure 3. Co-localization of Dorfin-30 immunoreactivity with Ub in neuronal and glial inclusions. Sections were doubly labeled with Dorfin antiserum and an antibody against Ub and analyzed with a laser-scanning confocal microscope. Panels at **left (green)** correspond to Ub, **middle** panels (**red**) correspond to Dorfin, and panels at **right** correspond to merged images; structures in yellow indicate co-localization. Dorfin is co-localized with Ub in ubiquitylated inclusions in the nigral neurons of PD (**A–F**), in glial cells in the putamen of MSA (**G–I**), and in spinal motor neurons of FALS (**J–L**). Co-localization of Dorfin and Ub is also seen in the pale body (**arrow**) and Lewy neurite (**asterisk**) in (**D–F**). Scale bar in **A** is equivalent to: 20 μm (**A-C** and **J–L**); 100 μm (**D–F**); 5 μm (**G–I**).

gated whether Dorfin is retained in high-molecular weight aggregates from α-synucleinopathy and ALS tissues by cellulose acetate filter trap assay. Homogenates of brain and spinal cord tissues from DLB, MSA, SALS, and controls were solubilized in TBS with 0.1% SDS, then filtered through a 0.22-μm cellulose acetate membrane. We have chosen the cerebral cortex for DLB, putamen for MSA, and the cerebral cortex and spinal cord for SALS for this assay, because these regions exhibit the most prominent pathology in each disease. Subsequent staining with Dorfin antiserum revealed trapped proteins (Figure 5A, top), which were also recognized by antibodies to Ub (Figure 5A, top middle). Furthermore, in DLB and MSA brains, α-synuclein was trapped, as expected (Figure 5A, bottom middle). Interestingly, high-molecular weight aggregates were difficult to detect in extracts of the cerebral cortex of SALS, in which pathological changes are less severe compared to those in the spinal cord. No high-molecular weight aggregate was present in either brain or spinal cord samples from normal control.

Sequential detergent extraction methods have been successfully applied to detect high-molecular weight complexes in brain of patients with α-synucleinopathies.[37,38] We used this method to detect insoluble Dorfin molecules in inclusion-rich tissues. Buffer- and Triton X-100-soluble ~98-kd and ~52-kd Dorfin were detected in brains from normal control as well as from DLB, MSA, and ALS patients (Figure 5B). In contrast to urea extracts of normal brain that were devoid of Dorfin immunoreactivities, ~98-kd full-length and ~52-kd truncated Dorfin were found in urea extracts from DLB, MSA, and ALS patients (Figure 5B). Bands, ~200 kd, ~45 kd and ~35 kd bands, were also detected (Figure 5B). These Dorfin-immunoreactive bands were not recognized by anti-Ub antibody (data not shown), and higher molecular weight bands may represent dimeric forms of Dorfin and smaller molecular weight species may be processed products of Dorfin.

These observations indicated that Dorfin is present in high-molecular weight structures in the tissues of α-synucleinopathy and ALS, suggesting that Dorfin is a major component of aggregated and ubiquitylated proteins forming inclusion bodies in these neurodegenerative disorders. Full-length Dorfin antigen is present in abnormal inclusions, but Triton-insoluble-urea-soluble higher molecular weight Dorfin and processed fragments seem to be major building blocks for inclusion bodies.

Dorfin Does Not Bind to Wild-Type and Mutant α-Synuclein

α-Synuclein is the main structural component of the insoluble protein aggregates that form the LBs of PD and DLB as well as the GCIs of MSA[37–39] and it has been shown to be ubiquitylated by an E3 Ub ligase, parkin.[40] As demonstrated, Dorfin is another major component of inclusion bodies in α-synucleinopathy, and because it has E3 activity,[9,10] we examined whether it interacts with α-synuclein *in vivo*. To this end, Xpress-tagged Dorfin was co-expressed with Myc-tagged wild-type or mutant forms of α-synuclein in HEK293 cells (Figure 6). In our experimental system, exogenously expressed α-synuclein was not phosphorylated (data not shown). Western blotting analysis after immunoprecipitation revealed that Dorfin binds with neither wild-type nor mutant α-synuclein. However, it strongly bound with mutant SOD1 (Figure 6), as we reported previously.[9] *In vitro* ubiquitylation assay using immunoprecipitated α-synuclein from transformed HEK293 cells, Dorfin did not ubiquitylate wild-type and mutant α-synuclein (data not shown).

Discussion

In the present study, we showed that Dorfin co-localizes to the ubiquitylated inclusions in common neurodegenerative diseases, including LBs in PD and DLB, GCIs in MSA, and hyaline and skein-like inclusions in ALS. Moreover, filter-trapped high-molecular weight structures contained Dorfin, indicating that it is a major constituent of these inclusions irrespective of the different disease etiologies and different morphological features of these inclusion bodies.

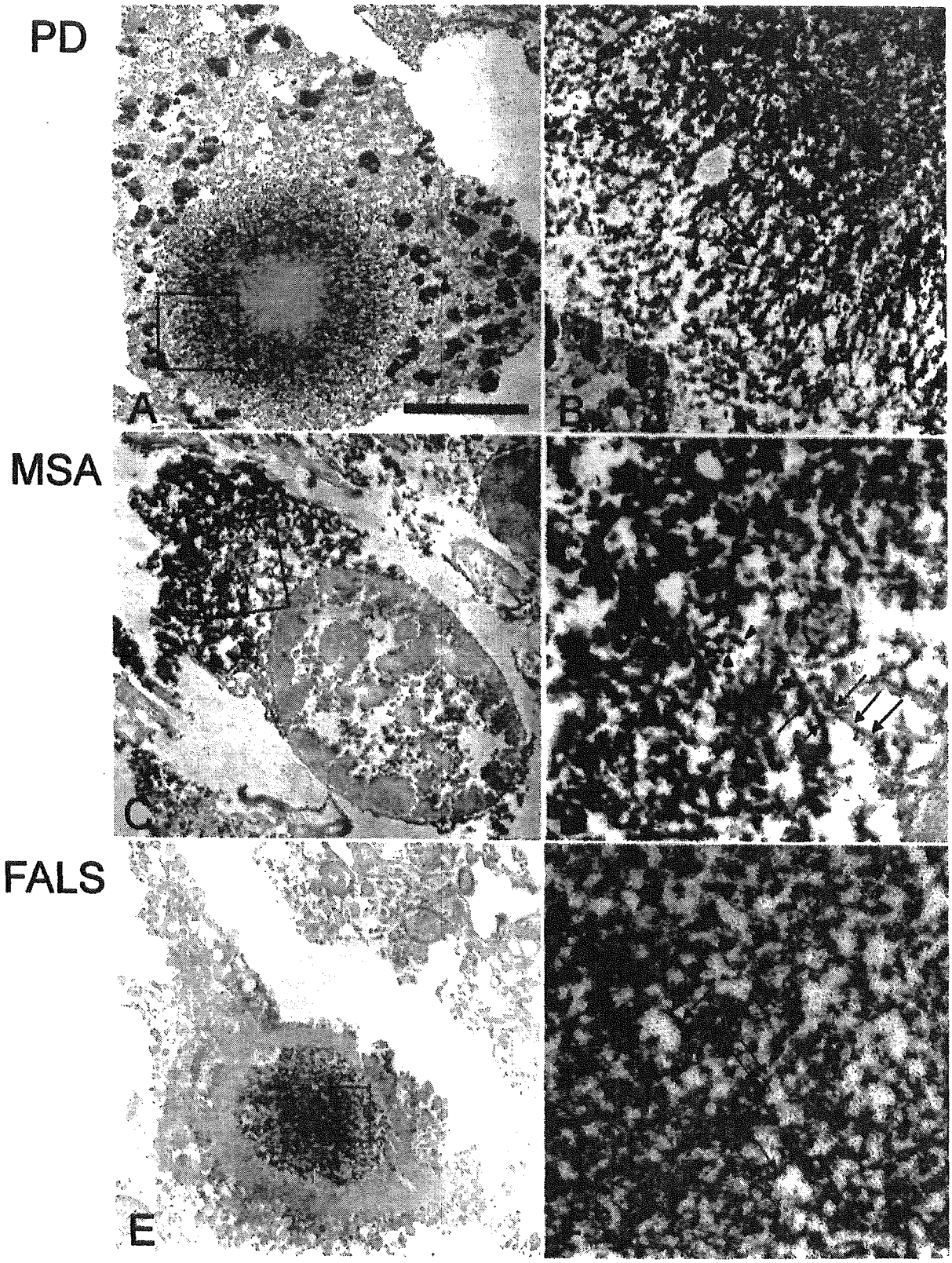

Figure 4. Immunoelectron microscopy of the neuronal and glial inclusions of PD, MSA, and FALS using the Dorfin-30 antibody. **A** and **B:** Typical LB immunostained with anti-Dorfin antibody in a pigmented neuron of substantia nigra in PD. The peripheral radiating filaments are strongly stained, and the central core is not Dorfin-immunoreactive. The immunoreactive filaments labeled with anti-Dorfin-30 antibody in **A** are shown at higher magnification (**arrows** in **B**) from area in the **square** in **A**. **B** shows that granular and fibrous materials are strongly positive for Dorfin, and are arranged radially. **C** and **D:** GCI of the oligodendrocyte is positive for Dorfin immunoreactivity in MSA. The granular materials (**arrowheads** in **D**) and the fibrous structures (**arrows** in **D**) are strongly stained with the Dorfin antibody from area in the **square** in **C**. **E** and **F:** LB-like hyaline inclusion in the spinal motor neurons in FALS. The filamentous structures (**arrows** in **F**) in the central core are strongly stained with anti-Dorfin antibody, but the filaments in the halo are not. **F** shows higher magnification of the central core region (**square**) in **E**. The granule-associated thick filaments are decorated. Scale bar in **A** is equivalent to: 5.5 μm (**A** and **E**); 2.5 μm (**C**); 0.8 μm (**B**); 0.83 μm (**D**); 0.85 μm (**F**).

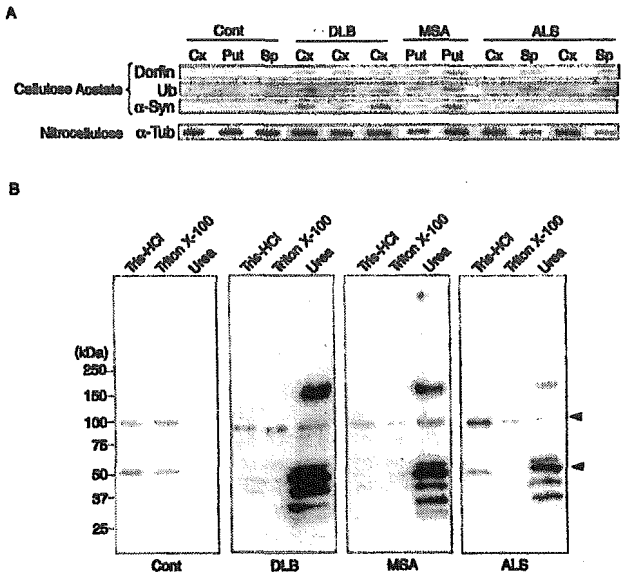

Figure 5. Dorfin accumulation in ubiquitylated high-molecular weight complexes. **A:** Detection of Dorfin in high-molecular weight structures in DLB, MSA, and SALS. Homogenates from brain and spinal cord of these diseases were filtered through cellulose acetate membranes and detected with Dorfin-30 antibody (**top**), anti-Ub antibody (**top middle**), and anti-α-synuclein antibody (**bottom middle**). Cx, cerebral cortex; Put, putamen; Sp, spinal cord. Nitrocellulose slot-blot probed with anti-α-tubulin antibody was used to confirm loading of equal amounts of samples (**bottom**). These results were replicated in duplicate experiments with different DLB, MSA, SALS, and control cases. **B:** Sequential extraction of Dorfin. Brains (normal, DLB, and MSA) and spinal cord (ALS) samples were sequentially extracted based on their solubility into Tris-HCl, Triton X-100, and urea buffers. Dorfin immunoreactivities were recovered in Tris and Triton fractions as ~98-kd and ~52-kd bands. In addition to these bands, Dorfin-30 antibody detected ~200-kd, ~45-kd, and ~35-kd bands in DLB, MSA, and ALS urea extracts, but not in normal brain urea extract. The **arrowheads** indicate ~98-kd full-length and ~52-kd truncated Dorfin bands.

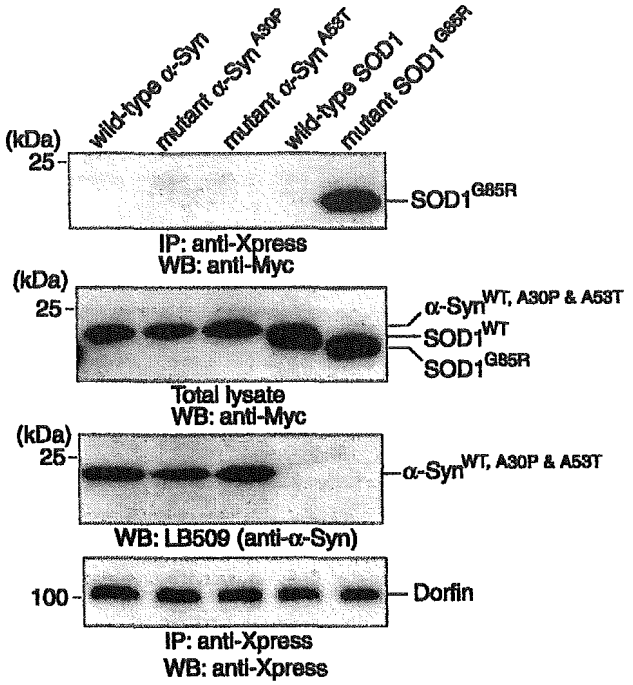

Figure 6. Dorfin binds to mutant SOD1 but not to α-synuclein. Myc-tagged wild-type and mutant α-synucleins were co-transfected with Xpress-tagged Dorfin into HEK293 cells. After immunoprecipitation with anti-Xpress antibody, the resulting precipitates were analyzed by Western blotting. Myc-tagged wild-type SOD1 and mutant $SOD1^{G85R}$ were used for negative and positive controls, respectively.

The following among our reported observations support the view that Dorfin plays an important role in the formation of ubiquitylated inclusion bodies in α-synucleinopathy and ALS: 1) the presence of Dorfin in the inclusion bodies of these diseases, 2) the parallel distribution patterns of Ub and Dorfin, 3) the perinuclear aggresome-like localization of Dorfin in cultured cells,[10] and 4) the E3 Ub ligase function of Dorfin and the resultant generation of mutant SOD1-(Ub)n conjugates.[9,10] The relation of Dorfin to α-synucleinopathies and ALS shows striking similarities to the relation between parkin and PD. Parkin, a gene product responsible for one of the most common forms of familial PD,[41] was shown to have E3 Ub ligase activity.[31,40,42–45] It was recently demonstrated that an *O*-glycosylated α-synuclein is the substrate of parkin,[40] and that parkin localizes to the LBs of sporadic PD and DLB.[30] A link between sporadic and familial PD through α-synuclein and parkin suggests that common molecular pathogenetic mechanisms underlie PD. The accumulation of toxic or undesired proteins in neurons may result from a primary failure of degradation systems, and could subsequently lead to neurodegeneration. Alternatively, the constant production of high levels of impaired proteins may become a burden on the protein degradation process through the Ub-proteasome pathway, gradually overwhelming the capacity of the proteasome to degrade toxic proteins and subsequently leading to the accumulation of ubiquitylated proteins and eventual neuronal cell death. Such a scenario is consistent with a recent report that impairment of the Ub-proteasome system is caused by protein aggregation.[46]

From this perspective, it is conceivable that familial and sporadic forms of ALS also share a common pathogenetic mechanism with PD involving the dysfunction of the Ub-proteasome pathway. In sporadic ALS, posttranslationally modified unknown substrates of Dorfin other than mutant SOD1 might accumulate in ubiquitylated form and play a role in the pathogenesis of the disease. Therefore, it is important to identify the protein(s) that is (are) the substrate(s) of the E3 activity of Dorfin for an understanding of the pathogenetic mechanism of sporadic ALS. In addition, substrates of Dorfin other than α-synuclein may play an important role in the pathogenesis of sporadic PD, DLB, and MSA, or a posttranslational modification (eg, glycosylation,[40] phosphorylation[47,48]) of α-synuclein may be necessary to be a substrate for Dorfin, because we failed to show the interaction between Dorfin and nonmodified α-synuclein overexpressed in HEK293 cells in this report. Furthermore, our findings raise the possibility that PD, DLB, MSA, and ALS are etiologically distinct, but share a biochemically common metabolic pathway through Dorfin leading to the formation of ubiquitylated inclusion bodies and to neuronal cell degeneration.

The generation of Dorfin knockout mice may determine whether Dorfin is essential to form ubiquitylated inclusion bodies and is indispensable to prevent neurons from the

toxic insult of protein aggregation. It may reveal what specific roles and relationships Dorfin and parkin have with one another as members of an E3 Ub ligase family containing a RING-finger/IBR domain.

References

1. Carrell RW, Lomas DA: Conformational disease. Lancet 1997, 350: 134–138
2. Johnson WG: Late-onset neurodegenerative diseases—the role of protein insolubility. J Anat 2000, 196:609–616
3. Mayer RJ, Lowe J, Lennox G, Doherty F, Landon M: Intermediate filaments and ubiquitin: a new thread in the understanding of chronic neurodegenerative diseases. Prog Clin Biol Res 1989, 317:809–818
4. Forno LS: Neuropathology of Parkinson's disease. J Neuropathol Exp Neurol 1996, 55:259–272
5. McKeith IG: Clinical Lewy body syndromes. Ann NY Acad Sci 2000, 920:1–8
6. Lantos PL: The definition of multiple system atrophy: a review of recent developments. J Neuropathol Exp Neurol 1998, 57:1099–1111
7. Hirano A: Neuropathology of ALS: an overview. Neurology 1996, 47:S63–S66
8. Ince PG, Lowe J, Shaw PJ: Amyotrophic lateral sclerosis: current issues in classification, pathogenesis and molecular pathology. Neuropathol Appl Neurobiol 1998, 24:104–117
9. Niwa J, Ishigaki S, Hishikawa N, Yamamoto M, Doyu M, Murata S, Tanaka K, Taniguchi N, Sobue G: Dorfin ubiquitylates mutant SOD1 and prevents mutant SOD1-mediated neurotoxicity. J Biol Chem 2002, 277:36793–36798
10. Niwa J, Ishigaki S, Doyu M, Suzuki T, Tanaka K, Sobue G: A novel centrosomal ring-finger protein, dorfin, mediates ubiquitin ligase activity. Biochem Biophys Res Commun 2001, 281:706–713
11. Morett E, Bork P: A novel transactivation domain in parkin. Trends Biochem Sci 1999, 24:229–231
12. Moynihan TP, Ardley HC, Nuber U, Rose SA, Jones PF, Markham AF, Scheffner M, Robinson PA: The ubiquitin-conjugating enzymes UbcH7 and UbcH8 interact with RING finger/IBR motif-containing domains of HHARI and H7-AP1. J Biol Chem 1999, 274:30963–30968
13. Ardley HC, Tan NG, Rose SA, Markham AF, Robinson PA: Features of the parkin/ariadne-like ubiquitin ligase, HHARI, that regulate its interaction with the ubiquitin-conjugating enzyme, Ubch7. J Biol Chem 2001, 276:19640–19647
14. Borchelt DR, Lee MK, Slunt HS, Guarnieri M, Xu ZS, Wong PC, Brown Jr RH, Price DL, Sisodia SS, Cleveland DW: Superoxide dismutase 1 with mutations linked to familial amyotrophic lateral sclerosis possesses significant activity. Proc Natl Acad Sci USA 1994, 91:8292–8296
15. Hoffman EK, Wilcox HM, Scott RW, Siman R: Proteasome inhibition enhances the stability of mouse Cu/Zn superoxide dismutase with mutations linked to familial amyotrophic lateral sclerosis. J Neurol Sci 1996, 139:15–20
16. McClellan AJ, Frydman J: Molecular chaperones and the art of recognizing a lost cause. Nat Cell Biol 2001, 3:E51–E53
17. Murata S, Minami Y, Minami M, Chiba T, Tanaka K: CHIP is a chaperone-dependent E3 ligase that ubiquitylates unfolded protein. EMBO Rep 2001, 2:1133–1138
18. Cyr DM, Hohfeld J, Patterson C: Protein quality control: u-box-containing E3 ubiquitin ligases join the fold. Trends Biochem Sci 2002, 27:368–375
19. Kopito RR: Aggresomes, inclusion bodies and protein aggregation. Trends Cell Biol 2000, 10:524–530
20. Johnston JA, Dalton MJ, Gurney ME, Kopito RR: Formation of high molecular weight complexes of mutant Cu,Zn-superoxide dismutase in a mouse model for familial amyotrophic lateral sclerosis. Proc Natl Acad Sci USA 2000, 97:12571–12576
21. McKeith IG, Galasko D, Kosaka K, Perry EK, Dickson DW, Hansen LA, Salmon DP, Lowe J, Mirra SS, Byrne EJ, Lennox G, Quinn NP, Edwardson JA, Ince PG, Bergeron C, Burns A, Miller BL, Lovestone S, Collerton D, Jansen EN, Ballard C, de Vos RA, Wilcock GK, Jellinger KA, Perry RH: Consensus guidelines for the clinical and pathologic diagnosis of dementia with Lewy bodies (DLB): report of the Consortium on DLB International Workshop. Neurology 1996, 47:1113–1124
22. Gilman S, Low PA, Quinn N, Albanese A, Ben-Shlomo Y, Fowler CJ, Kaufmann H, Klockgether T, Lang AE, Lantos PL, Litvan I, Mathias CJ, Oliver E, Robertson D, Schatz I, Wenning GK: Consensus statement on the diagnosis of multiple system atrophy. J Neurol Sci 1999, 163:94–98
23. Brooks BR: El Escorial World Federation of Neurology criteria for the diagnosis of amyotrophic lateral sclerosis. Subcommittee on Motor Neuron Diseases/Amyotrophic Lateral Sclerosis of the World Federation of Neurology Research Group on Neuromuscular Diseases and the El Escorial "Clinical Limits of Amyotrophic Lateral Sclerosis" Workshop Contributors. J Neurol Sci 1994, 124:S96–S107
24. Hishikawa N, Hashizume Y, Yoshida M, Sobue G: Widespread occurrence of argyrophilic glial inclusions in Parkinson's disease. Neuropathol Appl Neurobiol 2001, 27:362–372
25. Li M, Nakagomi Y, Kobayashi Y, Merry DE, Tanaka F, Doyu M, Mitsuma T, Hashizume Y, Fischbeck KH, Sobue G: Nonneural nuclear inclusions of androgen receptor protein in spinal and bulbar muscular atrophy. Am J Pathol 1998, 153:695–701
26. Li M, Miwa S, Kobayashi Y, Merry DE, Yamamoto M, Tanaka F, Doyu M, Hashizume Y, Fischbeck KH, Sobue G: Nuclear inclusions of the androgen receptor protein in spinal and bulbar muscular atrophy. Ann Neurol 1998, 44:249–254
27. Wang J, Xu G, Borchelt DR: High molecular weight complexes of mutant superoxide dismutase 1: age-dependent and tissue-specific accumulation. Neurobiol Dis 2002, 9:139–148
28. Lee M, Hyun D, Halliwell B, Jenner P: Effect of the overexpression of wild-type or mutant α-synuclein on cell susceptibility to insult. J Neurochem 2001, 76:998–1009
29. Parraga M, del Mazo J: XYbp, a novel RING-finger protein, is a component of the XY body of spermatocytes and centrosomes. Mech Dev 2000, 90:95–101
30. Schlossmacher MG, Frosch MP, Gai WP, Medina M, Sharma N, Forno L, Ochiishi T, Shimura H, Sharon R, Hattori N, Langston JW, Mizuno Y, Hyman BT, Selkoe DJ, Kosik KS: Parkin localizes to the Lewy bodies of Parkinson disease and dementia with Lewy bodies. Am J Pathol 2002, 160:1655–1667
31. Imai Y, Soda M, Inoue H, Hattori N, Mizuno Y, Takahashi R: An unfolded putative transmembrane polypeptide, which can lead to endoplasmic reticulum stress, is a substrate of Parkin. Cell 2001, 105:891–902
32. Imai Y, Soda M, Hatakeyama S, Akagi T, Hashikawa T, Nakayama KI, Takahashi R: CHIP is associated with Parkin, a gene responsible for familial Parkinson's disease, and enhances its ubiquitin ligase activity. Mol Cell 2002, 10:55–67
33. Gai WP, Yuan HX, Li XQ, Power JT, Blumbergs PC, Jensen PH: In situ and in vitro study of colocalization and segregation of alpha-synuclein, ubiquitin, and lipids in Lewy bodies. Exp Neurol 2000, 166:324–333
34. Takahashi H, Wakabayashi K: The cellular pathology of Parkinson's disease. Neuropathology 2001, 21:315–322
35. Scherzinger E, Lurz R, Turmaine M, Mangiarini L, Hollenbach B, Hasenbank R, Bates GP, Davies SW, Lehrach H, Wanker EE: Huntingtin-encoded polyglutamine expansions form amyloid-like protein aggregates in vitro and in vivo. Cell 1997, 90:549–558
36. Bailey CK, Andriola IF, Kampinga HH, Merry DE: Molecular chaperones enhance the degradation of expanded polyglutamine repeat androgen receptor in a cellular model of spinal and bulbar muscular atrophy. Hum Mol Genet 2002, 11:515–523
37. Baba M, Nakajo S, Tu PH, Tomita T, Nakaya K, Lee VM, Trojanowski JQ, Iwatsubo T: Aggregation of α-synuclein in Lewy bodies of sporadic Parkinson's disease and dementia with Lewy bodies. Am J Pathol 1998, 152:879–884
38. Dickson DW, Liu W, Hardy J, Farrer M, Mehta N, Uitti R, Mark M, Zimmerman T, Golbe L, Sage J, Sima A, D'Amato C, Albin R, Gilman S, Yen SH: Widespread alterations of α-synuclein in multiple system atrophy. Am J Pathol 1999, 155:1241–1251
39. Spillantini MG, Crowther RA, Jakes R, Hasegawa M, Goedert M: α-Synuclein in filamentous inclusions of Lewy bodies from Parkinson's disease and dementia with Lewy bodies. Proc Natl Acad Sci USA 1998, 95:6469–6473

40. Shimura H, Schlossmacher MG, Hattori N, Frosch MP, Trockenbacher A, Schneider R, Mizuno Y, Kosik KS, Selkoe DJ: Ubiquitination of a new form of α-synuclein by parkin from human brain: implications for Parkinson's disease. Science 2001, 293:263–269
41. Kitada T, Asakawa S, Hattori N, Matsumine H, Yamamura Y, Minoshima S, Yokochi M, Mizuno Y, Shimizu N: Mutations in the parkin gene cause autosomal recessive juvenile parkinsonism. Nature 1998, 392:605–608
42. Shimura H, Hattori N, Kubo S, Mizuno Y, Asakawa S, Minoshima S, Shimizu N, Iwai K, Chiba T, Tanaka K, Suzuki T: Familial Parkinson disease gene product, parkin, is a ubiquitin-protein ligase. Nat Genet 2000, 25:302–305
43. Imai Y, Soda M, Takahashi R: Parkin suppresses unfolded protein stress-induced cell death through its E3 ubiquitin-protein ligase activity. J Biol Chem 2000, 275:35661–35664
44. Zhang Y, Gao J, Chung KK, Huang H, Dawson VL, Dawson TM: Parkin functions as an E2-dependent ubiquitin-protein ligase and promotes the degradation of the synaptic vesicle-associated protein, CDCrel-1. Proc Natl Acad Sci USA 2000, 97:13354–13359
45. Chung KK, Zhang Y, Lim KL, Tanaka Y, Huang H, Gao J, Ross CA, Dawson VL, Dawson TM: Parkin ubiquitinates the α-synuclein-interacting protein, synphilin-1: implications for Lewy-body formation in Parkinson disease. Nat Med 2001, 7:1144–1150
46. Bence NF, Sampat RM, Kopito RR: Impairment of the ubiquitin-proteasome system by protein aggregation. Science 2001, 292: 1552–1555
47. Okochi M, Walter J, Koyama A, Nakajo S, Baba M, Iwatsubo T, Meijer L, Kahle PJ, Haass C: Constitutive phosphorylation of the Parkinson's disease associated α-synuclein. J Biol Chem 2000, 275: 390–397
48. Fujiwara H, Hasegawa M, Dohmae N, Kawashima A, Masliah E, Goldberg MS, Shen J, Takio K, Iwatsubo T: α-Synuclein is phosphorylated in synucleinopathy lesions. Nat Cell Biol 2002, 4:160–164

DOI: 10.1093/brain/awg012 *Brain* (2003), **126**, 134–151

Demyelinating and axonal features of Charcot–Marie–Tooth disease with mutations of myelin-related proteins (PMP22, MPZ and Cx32): a clinicopathological study of 205 Japanese patients

Naoki Hattori,[1] Masahiko Yamamoto,[1] Tsuyoshi Yoshihara,[1] Haruki Koike,[1] Masanori Nakagawa,[2] Hiroo Yoshikawa,[3] Akio Ohnishi,[4] Kiyoshi Hayasaka,[5] Osamu Onodera,[6] Masayuki Baba,[7] Hitoshi Yasuda,[8] Toyokazu Saito,[9] Kenji Nakashima,[10] Jun-ichi Kira,[11] Ryuji Kaji,[12] Nobuyuki Oka[13] Gen Sobue[1] and and the Study Group for Hereditary Neuropathy in Japan

[1]Department of Neurology, Nagoya University Graduate School of Medicine, Nagoya, [2]Third Department of Internal Medicine, Kagoshima University Faculty of Medicine, Kagoshima, [3]Department of Neurology, Osaka Kosei-Nenkin Hospital, Osaka, [4]Department of Neurology, School of Medicine, University of Occupational and Environmental Health, Kitakyushu, [5]Department of Pediatrics, Yamagata University School of Medicine, Yamagata, [6]Department of Neurology, Niigata University Graduate School of Medicine and Dental Sciences, Niigata, [7]Department of Neurology, Hirosaki University School of Medicine, Hirosaki, [8]Third Department of Internal Medicine, Shiga University of Medical Science, Otsu, [9]Department of Neurology, Kitasato University School of Medicine, Sagamihara, [10]Department of Neurology, Tottori University Faculty of Medicine, Yonago, [11]Department of Neurology, Kyushu University Graduate School of Medicine, Fukuoka, [12]Division of Advanced Clinical Neuroscience, University of Tokushima School of Medicine, Tokushima and [13]Department of Internal Medicine, Hyogo College of Medicine, Nishinomiya, Japan

Correspondence to: Gen Sobue, MD, Department of Neurology, Nagoya University Graduate School of Medicine, 65 Tsurumai-cho Showa-ku Nagoya 466 8550, Japan
E-mail: sobueg@tsuru.med.nagoya-u.ac.jp

Summary

Three genes commonly causing Charcot–Marie–Tooth disease (CMT) encode myelin-related proteins: peripheral myelin protein 22 (PMP22), myelin protein zero (MPZ) and connexin 32 (Cx32). Demyelinating versus axonal phenotypes are major issues in CMT associated with mutations of these genes. We electrophysiologically, pathologically and genetically evaluated demyelinating and axonal features of 205 Japanese patients with PMP22 duplication, MPZ mutations or Cx32 mutations. PMP22 duplication caused mainly demyelinating phenotypes with slowed motor nerve conduction velocity (MCV) and demyelinating histopathology, while axonal features were variably present. Two distinctive phenotypic subgroups were present in patients with MPZ mutations: one showed preserved MCV and exclusively axonal pathological features, while the other was exclusively demyelinating. These axonal and demyelinating phenotypes were well concordant among siblings in individual families, and MPZ mutations did not overlap among these two subgroups, suggesting that the nature and position of the MPZ mutations mainly determine the axonal and demyelinating phenotypes. Patients with Cx32 mutations showed intermediate slowing of MCV, predominantly axonal features and relatively mild demyelinating pathology. These axonal and demyelinating features were present concomitantly in individual patients to a variable extent. The relative severity of axonal and demyelinating features was not associated with

particular Cx32 mutations. Median nerve MCV and overall histopathological phenotype changed little with disease advancement. Axonal features of diminished amplitudes of compound muscle action potentials (CMAPs), axonal loss, axonal sprouting and neuropathic muscle wasting all changed as disease advanced, especially in PMP22 duplication and Cx32 mutations. Median nerve MCVs were well maintained independently of age, disease duration and the severity of clinical and pathological abnormalities, confirming that median nerve MCV is an excellent marker for the genetically determined neuropathic phenotypes. Amplitude of CMAPs was correlated significantly with distal muscle strength in PMP22 duplication, MPZ mutations and Cx32 mutations, while MCV slowing was not, indicating that clinical weakness results from reduced numbers of functional large axons, not from demyelination. Thus, the three major myelin-related protein mutations induced varied degrees of axonal and demyelinating phenotypic features according to the specific gene mutation as well as the stage of disease advancement, while clinically evident muscle wasting was attributable to loss of functioning large axons.

Keywords: Charcot–Marie–Tooth disease; PMP22; MPZ; Cx32

Abbreviations: CK = creatine kinase; CMAP = compound muscle action potential; CMT = Charcot–Marie–Tooth disease; Cx32 = connexin 32; DL = distal latency; MCV = motor nerve conduction velocity; MPZ = myelin protein zero; PMP22 = peripheral myelin protein 22; SCV = sensory nerve conduction velocity; SNAP = sensory nerve action potential

Introduction

Charcot–Marie–Tooth disease (CMT) refers to a pathologically and genetically heterogeneous group of motor and sensory neuropathies characterized by slowly progressive weakness, muscle atrophy and sensory impairment, all most marked in the distal part of the legs. Two major phenotypes have been distinguished (Dyck and Lambert, 1968; Buchthal and Behse, 1977; Harding and Thomas, 1980). Type 1 (CMT1), the demyelinating form of CMT, results in a marked decrease in nerve conduction velocity (NCV) and segmental demyelination of peripheral nerves; type 2 (CMT2), the axonal form of CMT, shows primarily axonal involvement, with normal or slightly decreased NCV, as well as nerve fibre loss and axonal sprouting. In addition, a group showing features intermediate between those of types 1 and 2 has also been described (Bradley *et al.*, 1977). Many causative genes have been identified, prompting proposals for a new classification (Harding, 1995; Kamholz *et al.*, 2000; Reilly, 2000). Heterozygous duplication of the locus for the peripheral nerve myelin protein 22 (PMP22) gene on chromosome 17p11.2 is found in most patients with demyelinating CMT1A (Lupski *et al.*, 1991; Raeymaekers *et al.*, 1991; Matsunami *et al.*, 1992; Patel *et al.*, 1992; Timmerman *et al.*, 1992). Occasionally, a point mutation in the PMP22 gene rather than duplication is found in CMT1A patients (Nelis *et al.*, 1996; Kovach *et al.*, 1999). CMT1B, another demyelinating form, has been found to result from mutations in the myelin protein zero (MPZ) gene (Hayasaka *et al.*, 1993). Disease in another group of patients results from mutations of the connexin 32 (Cx32) gene (Bergoffen *et al.*, 1993; Ionasescu *et al.*, 1994, 1996). These three genes encoding myelin-related proteins are the major causes of CMT with demyelination. Recently, rare gene mutations in the early growth response protein (EGR2), myotubularin-related protein 2 (MTMR2), N-myc downstream-regulated gene 1 (NDRG-1), periaxin (PRX) and ganglioside-induced differentiation-associated protein 1 (GDAP1) genes have been found in patients with the demyelinating form (Warner *et al.*, 1998; Bolino *et al.*, 2000; Kalaydjieva *et al.*, 2000; Guilbot *et al.*, 2001; Nagarajan *et al.*, 2001; Yoshihara *et al.*, 2001; Baxter *et al.*, 2002). Several genes causing CMT type 2 have also been identified, including neurofilament L (NF-L) the kinesin motor superfamily (KIF1Bb) and lamin A/C nuclear envelope proteins, as well as GDAP1 (Mersiyanova *et al.*, 2000; Zhao *et al.*, 2001; De Sandre-Giovannoli *et al.*, 2002; Cuesta *et al.*, 2002).

CMT phenotypes caused by different gene abnormalities have been widely analysed, but no firm consensus has been established (Boerkoel *et al.*, 2002). In patients with Cx32 mutations, some authors considered the demyelinating process to predominate (Scherer, 1999; Scherer and Fischbeck, 1999; Tabaraud *et al.*, 1999; Gutierrez *et al.*, 2000), while others favoured a primarily axonal neuropathy (Hahn *et al.*, 1990, 2001; Birouk *et al.*, 1998; Senderek *et al.*, 1999). As for MPZ mutations, several families with an axonal phenotype have been reported (Gabreels-Festen *et al.*, 1996; Marrosu *et al.*, 1998; Chapon *et al.*, 1999; De Jonghe *et al.*, 1999; Misu *et al.*, 2000; Boerkoel *et al.*, 2002), suggesting a subgroup of patients with MPZ mutations causing a primarily axonal neuropathy. Wide variation has been shown in pathological findings, nerve conduction data, axonal and demyelinating severity, associated symptoms and prognosis in patients with MPZ, Cx32 and PMP22 gene abnormalities (Killian *et al.*, 1996; Birouk *et al.*, 1997, 1998; Thomas *et al.*, 1997; Senderek *et al.*, 1999; Dubourg *et al.*, 2001*a*; Boerkoel *et al.*, 2002). Phenotypic variation and the underlying gene abnormalities remain to be defined.

Axonal involvement has been reported in CMT1A, a demyelinating form (Dyck *et al.*, 1989; Garcia *et al.*, 1998; Krajewski *et al.*, 2000), as evidenced by decreased amplitude of muscle action potentials and by pathological abnormalities

(Dyck *et al.*, 1993; Garcia *et al.*, 1998; Krajewski *et al.*, 2000). In CMT1 patients, axonal involvement progressed in a time-dependent manner during a longitudinal study (Dyck *et al.*, 1989). Furthermore, conduction velocity and amplitude or neuropathic deficits at the first and last examinations in CMT1 were significantly correlated, suggesting an association between early slowing of conduction and subsequent neuropathic disability (Dyck *et al.*, 1989). These observations suggest that axonal involvement related to disease progression in demyelinating neuropathy is clinically important. However, demyelinating and axonal features that alter as disease progresses have not been assessed conclusively in CMT, particularly in forms other than CMT1A.

In addition, most studies of CMT phenotypic–genotypic variation have been performed in Caucasian populations; thus, features of CMT phenotypic–genotypic variation in Asian populations have not been elucidated. The frequency distribution of the breakpoint for PMP22 duplication at the CMT1A-REP (repeat) in 17p11.2 has been documented to be very similar among Caucasian and Asian populations (Yamamoto *et al.*, 1997), while the prevalence of CMT1A in the Japanese population has been considered to be extremely low compared with frequencies in Caucasians, although definitive comparative epidemiological studies have not been reported.

We therefore conducted a clinical, electrophysiological, histopathological and genetic study of 205 Japanese CMT patients with one of the three most common causative gene abnormalities, viz. abnormalities of PMP22, MPZ and Cx32, which involve major myelin-related proteins. We focused particularly on the demyelinating and axonal phenotypic features of these CMT patients.

Patients and methods

Patients and DNA diagnosis

Two hundred and five CMT patients from 124 families with a DNA diagnosis of PMP22 duplication (118 patients from 74 families), MPZ mutations (45 patients from 26 families) or Cx32 mutations (42 patients from 24 families; male only) were registered by the Study Group for Hereditary Neuropathy in Japan, working under the auspices of the Ministry of Health, Labour and Welfare of Japan. In the case of Cx32 mutations, gender effects on phenotypic expression are known to be profound (Nicholson and Nash, 1993; Birouk *et al.*, 1998; Dubourg *et al.*, 2001*b*), so only male patients were selected for our genotype–phenotype analysis. DNA analysis was performed in the Department of Neurology, Nagoya University Graduate School of Medicine, the Department of Pediatrics, Yamagata University School of Medicine, the Department of Neurology, Kagoshima University School of Medicine, or the Department of Neurology, Osaka University School of Medicine. In most cases, the PMP22 duplication was detected by Southern analysis, probing with PMP22 cDNA, the polymorphic markers VAW409R3 and EW401, and the CMT1A-REP fragments (Ikegami *et al.*, 1997; Yamamoto *et al.*, 1997, 1998). Hybridization with the probes pNEA102, pHK1.0P and pHK5.2P, mapping within the CMT1A-REP, was used to determine the location of crossover breakpoints, which were clustered in a 700-base pair (bp) region of the CMT1A-REP. Quantitation of hybridized signals for each band was performed to evaluate duplicate gene dosage using a phosphor-image analyser (BAS-2000II; Fujix, Tokyo, Japan). In some cases, fluorescence *in situ* hybridization (FISH) was employed to detect PMP22 gene duplication.

A non-isotopic RNase cleavage assay (NIRCA) was employed as a screening test for MPZ and Cx32 mutations using a method described previously (Yoshihara *et al.*, 2000). The MPZ and Cx32 genes, separated into three and two fragments respectively, were amplified with the polymerase chain reaction (PCR). Sequences of the forward (F) and reverse (R) primers were as follows:

For the MPZ gene: F1, 5′-CTA GGG ATT TTA AGC AGG TTC C-3′ and R1, 5′-ATT GCT GAG AGA CAC CTG AGT CC-3′ for exon 1; F2, 5′-CCA TAG GTG CAT CTG ATT CC-3′ and R2, 5′-CCT CCT TAG CCC AAT TTA TC-3′ for exon 2; and F3, 5′-CAG CTG TGT TCT CAT TAG GGT CCT C-3′ and R3, 5′-GCT CAT CCT TTC GTA GCT CCA TCT C-3′ for exons 3–6. For the Cx32 gene: F4, 5′-AGT GAC AGG GAG GTG TGA ATG AG-3′ and R4, 5′-AGG GGT AGA CGT CGC ACT TGA C-3′ for part 1 of exon 2; and F5, 5′-TTT GAG GCC GTC TTC ATG TAT GTC-3′ and R5, 5′-AGT AGC CAG GGA AGG AAG GTT TTG-3′ for part 2 of exon 2.

The bacteriophage T7 promoter sequence 5′-TAA TAC GAC TCA CTA TAG GG-3′ was attached to each primer at the 5′ end. PCR amplification was performed using AmpliTaq Gold (Perkin Elmer, Wellesley, MA, USA). Initial amplification conditions were 95°C for 9 min for denaturation, followed by 35 cycles of denaturing at 95°C for 1 min, annealing at 60°C for 1 min and elongation at 72°C for 2 min. NIRCA was performed using a MutationScreener kit (Ambion, Austin, TX, USA) according to the manufacturer's protocol. This assay system is based on the properties of the RNase enzyme that cleaves single base-pair mismatches of hybridized RNA duplexes produced *in vitro* by generating sense and antisense transcripts of each PCR product using the specific primer pairs. The bacteriophage RNA T7 promoter sequence integrated into the forward and reverse primers allowed the PCR products to be converted to RNA. Sense and antisense RNA transcripts were hybridized, and RNA–RNA hybrids were then treated with an optimized RNase mixture (RNase I and RNase T1) to cleave the duplexes at the mismatch positions. RNase-digested products were electrophoresed through 2.5% agarose gels. PCR products were purified from the unreacted primers and nucleotides using a QIAquick PCR Purification kit (Qiagen, Valencia, CA, USA) according to the manufacturer's protocol. Duplicate amplifications analysed by NIRCA were performed to avoid false-positive results arising from PCR errors. Purified products

Table 1 *Clinical features in 205 CMT patients with PMP22 duplication, MPZ mutations and Cx32 mutations*

Clinical features	PMP22 duplication	MPZ mutations			Cx32 mutations
		Total	MCV ⩽38 m/s	MCV >38 m/s	
	(n = 118)	(n = 45)	(n = 28)	(n = 17)	(n = 42)
Age (years)	44.5 ± 19.2	36.9 ± 15.1	30.3 ± 15.1	48.8 ± 24.5	43.2 ± 21.4
Age of onset (years)	20.3 ± 16.3	20.9 ± 23.3	13.2 ± 15.3	34.0 ± 24.8	22.4 ± 19.0
Disease duration (years)	22.7 ± 17.3	15.2 ± 10.7	17.1 ± 13.5	14.8 ± 11.9	17.5 ± 19.8
Sex, male/female (n)	58/60	20/35	13/15	7/10	42/0
Muscle weakness: n (%)	118 (100)	45 (100)	28 (100)	17 (100)	42 (100)
Muscular atrophy: n (%)	98 (83)	39 (86)	24 (86)	15 (88)	36 (86)
Muscular hypertrophy: n (%)	5 (4)	3 (7)	2 (7)	1 (6)	0 (0)
Sensory impairment: n (%)	105 (89)	40 (89)	25 (89)	15 (88)	36 (86)
Areflexia: n (%)	118 (100)	32 (71)	22 (78)	10 (59)	34 (81)
Associated symptoms: n (%)					
Deafness	2 (2)	7 (16)	2 (7)	5 (29)	4 (9)
Pupillary abnormality	0 (0)	8 (18)	2 (7)	6 (35)	3 (7)
Scoliosis	6 (5)	6 (13)	3 (11)	3 (17)	2 (5)
Dementia	0 (0)	0 (0)	0 (0)	0 (0)	1 (2)
Serum CK elevation: n (%)	4 (3)	14 (30)	6 (21)	8 (47)	9 (21)
CSF protein elevation: n (%)	61 (52)	34 (76)	21 (75)	13 (76)	16 (38)
ADL score (modified Rankin score): n (%)					
0	74 (62)	22 (50)	15 (53)	7 (41)	4 (9)
1	32 (26)	11 (24)	9 (32)	2 (12)	30 (72)
2	5 (6)	5 (11)	3 (11)	2 (12)	2 (5)
3	4 (5)	6 (13)	1 (4)	5 (29)	3 (7)
4	1 (1)	1 (2)	0 (0)	1 (6)	3 (7)
5	0 (0)	0 (0)	0 (0)	0 (0)	0 (0)

For Cx32 mutations, male patients were selected. ADL = activities of daily living.

were sequenced directly using a Thermo Sequenase Cy5.5 terminator cycle sequencing kit (Amersham Biosciences, Piscataway, NJ, USA) and analysed with a GeneRapid sequencer system (Amersham, Pharmacia). In some cases, FISH was employed to detect PMP22 gene duplication. As the patients with point mutations of the PMP22 gene are not included in this paper, 'PMP22 mutation' means 'PMP22 duplication'.

Informed consent was granted by subjects beforehand according to the guidelines of the Ethics Committee of Nagoya University Graduate School of Medicine or those of the regional ethics committee for each institution.

Clinical assessment

Clinical information was assessed in a standardized manner, including motor and sensory impairment, deep tendon reflexes, muscular atrophy or hypertrophy, foot deformity and autonomic impairment. Weakness was assessed in proximal muscles (deltoid, biceps, triceps muscles in the arm; iliopsoas, quadriceps muscles in the legs) as well as distal muscles (thenar, interosseous, finger flexion muscles in the arms; ankle dorsiflexion and toe dorsiflexion muscles in the legs) according to UK Medical Research Council (MRC) criteria (Hattori *et al.*, 1999). Impairment was assessed for various sensory modalities (vibration, joint position, pain and light touch) as mild, moderate or severe. Associated findings, including deafness, pupillary abnormalities, scoliosis and dementia, were also assessed. Routine blood chemistry results were reviewed, as were those of CSF analysis and cranial and limb MRI. Detailed family histories were obtained.

Ability to carry out activities of daily living was evaluated according to the modified Rankin scale as follows: 0, normal; 1, non-disabling symptoms not interfering with lifestyle; 2, minor disability from symptoms leading to some restrictions of lifestyle but not interfering with patients' capacity to look after themselves; 3, moderate disability from symptoms that significantly interfered with lifestyle or prevented fully independent existence; 4, moderately severe disability from symptoms that clearly precluded independent existence, although patients did not need constant attention day and night; 5, severe disability involving total dependence, including constant care day and night.

Electrophysiological analysis

Nerve conduction was assessed for the median, ulnar, tibial and sural nerves. Recordings were performed by standard methods using surface stimulating and recording electrodes (Hattori *et al.*, 1999; Misu *et al.*, 1999, 2000; Koike *et al.*, 2001). Motor nerve conduction velocity (MCV), distal motor latency (DL) and compound muscle action potential (CMAP) were recorded for the median, ulnar and tibial nerves. Sensory nerve conduction velocity (SCV) and sensory nerve action potential (SNAP) were assessed for the median and sural nerves.